Biogeochemistry (2007) 86:33–62
DOI 10.1007/s10533-007-9143-x

ORIGINAL PAPER

Spatial variation of redox and trace metal geochemistry in a minerotrophic fen

Carla M. Koretsky · Melanie Haveman · Lauren Beuving · Angel Cuellar · Terri Shattuck · Mark Wagner

Received: 28 February 2007 / Accepted: 25 June 2007 / Published online: 27 July 2007

Abstract Pore water and solid phase samples were collected from the upper 50 cm of a peat profile at four sites within a 10 m^2 area in Kleinstuck Marsh, a minerotropic fen located in Kalamazoo, MI. Although the chosen sites are in close proximity to each other, they differ with respect to vegetation species and density. Pore water analyses for a suite of redox sensitive species (pH, alkalinity, dissolved Mn(II), Fe(II), Fe(III), sulfide, sulfate), together with Fe and Mn distributions inferred from operationally-defined sequential extractions, demonstrate that Fe(III) and Mn(IV) reduction occurs in the shallow peat at three of the four sites. At the fourth site, the only site containing the invasive purple loosestrife (*Lythrum salicaria*), accumulation of dissolved sulfide in the pore waters and increased levels of oxidizable phases in the shallow peat point to increased net sulfate reduction relative to the other three sites. Speciation calculations indicate that pore water concentrations of phosphate, especially below ~10 cm depth, are largely controlled by the solubility of phases such as strengite or hydroxylapatite, and that at all but the loosestrife site, dissolved Ca and Mg are likely determined by carbonate solubility. Fe and Mn distribution among operationally defined solid phase fractions are consistent with reductive dissolution of FMO in the uppermost peat, leading to precipitation of Fe sulfides and Mn carbonates deeper in the peat profile. Zn, Co, Cr and Ni distributions are consistent with release from FMO to form sulfides or organic associations deeper in the peat. Pb and Cu may also be released by reductive dissolution of FMO, or more likely, shift from primary association with organic matter to increased association with sulfides under more sulfidic conditions. This study highlights the existence of extreme lateral variations in peat pore water and solid phase geochemical profiles, even over quite small areas.

Keywords Pore water geochemistry · Redox stratification · Sediment extraction · Sequential extraction · Trace metal · Macrophyte

C. M. Koretsky (✉) · M. Haveman · L. Beuving · A. Cuellar · T. Shattuck · M. Wagner
Department of Geosciences, Environmental Studies Program, Western Michigan University, Kalamazoo, MI 49008, USA
e-mail: carla.koretsky@wmich.edu

Introduction

Freshwater wetlands play a vital role in fostering biological diversity, providing wildlife habitat, mitigating drought and flooding, reducing soil erosion, recharging groundwater aquifers, and in the biogeochemical cycling of phosphorus, nitrogen, carbon and sulfur (Mitsch and Gosselink 2000). For example, much research has focused on nutrient transformations within wetlands and the potential for wetlands to act as long-term sinks for phosphorus and nitrogen

(e.g., Johnston 1991; Arheimer and Wittgren 2002; Day et al. 2004; Hogan et al. 2004; Mungasavalli and Viraraghavan 2006; Verhoeven et al. 2006). Because many wetlands are highly productive and have the potential to store or release large quantities of carbon, their influence on global climate change is of great interest (e.g., Brix et al. 2001; Shindell et al. 2004; Ellis and Rochefort 2006; Smemo and Yavitt 2006; Tarnocai 2006; Trettin et al. 2006). Freshwater peat sediments have also been demonstrated to host dynamic cycles of S transformations (e.g., Wieder and Lang 1988; Wieder et al. 1990; Keller and Bridgham 2007; Blodau et al. 2007). The connection between changes in S concentration, for example induced by increased anthropogenic atmospheric deposition, and changes in microbial pathways and carbon processing are poorly understood at present (Wieder et al. 1990; Watson and Nedwell 1998; Dise and Verry 2001; Gauci et al. 2004). Less attention has typically been focused on trace metal-cycling within peats, especially in minerotrophic systems, although anthropogenic addition of metals to wetlands via atmospheric deposition, surface runoff, and direct dumping is common (Crowder 1991; Mitsch and Gosselink 2000). Significant efforts have been made to use peat-accumulating wetlands to gain historical records of anthropogenic trace metal deposition (Shotyk 1996; Shotyk et al. 1997). However, these efforts are complicated by early diagenetic processes, which can remobilize metals within sediments and soils (Norton 1987; Gambrell 1994; Hamilton-Taylor and Davison 1995; Shotyk 1996; Perkins et al. 2000; Rausch et al. 2005).

Post-depositional remobilization of trace metals, carbon processing, and nutrient transformations all depend on factors including wetland hydrology, geomorphology, climate and the activities of various types of macrofauna and macrophytes. Many of these influence wetland soil oxidation–reduction (redox) chemistry. Wetland soils are redox stratified, meaning that a sequence of vertical zones can be delineated based on pore water and solid phase geochemistry (e.g., Koretsky et al. 2006a; CM Koretsky et al. submitted). In organic-rich, water-saturated wetlands, O_2 concentrations decrease rapidly with depth. For example, in saltmarsh sediments, microelectrodes have been used to show that O_2 penetration is typically limited to the upper few mm of the sediment column (Brendel and Luther 1995). Within this thin oxic zone, oxygen can be consumed by aerobic respiration or via oxidation of reduced chemical species, such as ammonia, Mn(II) or Fe(II), diffusing upwards from deeper, more reduced layers. Below the oxic zone lies the suboxic zone, where dissolved Mn(II) and Fe(II) are produced by the reductive dissolution of relatively insoluble Fe(III) and Mn(IV) hydroxide phases (FMO). Such reactions can either occur abiotically, for example, reduction of Fe(III) coupled to oxidation of H_2S, or microbially, by dissimilatory iron and manganese reduction (Lovley and Philips 1986; Myers and Nealson 1988; dos Santos Afonso and Stumm 1992; Yao and Millero 1996; Lowe et al. 2000; Roden and Wetzel 2002; Koretsky et al. 2003). Beneath the suboxic zone, organic matter degradation is coupled primarily to sulfate reduction. In this sulfidic zone, dissolved sulfide accumulates in the pore waters or as solid metal sulfide phases. The relative sizes of the oxic, suboxic and sulfidic zones are determined by reaction rates together with the quantity of available labile organic carbon and the availability of terminal electron acceptors (e.g., O_2, Mn(IV), Fe(III), sulfate). Zones can thin in response to increased reaction rates, for example during warmer seasons, or in response to increases in labile organic carbon availability. Transport processes, including advective flow, as well as non-local solute transport via macrofaunal pumping of surface waters into the subsurface via burrows (bioirrigation) or leakage of O_2 into the rhizosphere surrounding macrophyte roots, can lead to broader zones with less compressed redox stratification (Koretsky et al. 2003, 2005, 2006a, b).

Changes in redox stratification play an important role in trace metal distribution (Balistrieri et al. 1992a, b; Davison 1993; Hamilton-Taylor and Davison 1995; Gambrell 1994; Tessier et al. 1996; Achterberg et al. 1997; Boudreau 1999; Weis and Weis 2004: Koretsky et al. 2006a, b; CM Koretsky et al. submitted), and therefore in metal mobility and bioavailability, which depend strongly on speciation (Sunda and Guillard 1976; Allen et al. 1980; Campbell 1995; Deighton and Goodman 1995). FMO, which are formed under oxic conditions and are reductively dissolved in the suboxic zone, can sequester trace metals, both via adsorption and coprecipitation (Dzombak and Morel 1990; Hamilton-Taylor and Davison 1995; Tonkin et al. 2004). Thus, reductive dissolution can release not only

dissolved Mn(II) and Fe(II) to pore waters, but also associated trace metals, potentially making them more bioavailable and mobile (Balistrieri et al. 1992a, b; Kerner and Wallmann 1992; Davison 1993; Tessier et al. 1996; Hamilton-Taylor et al. 1999; Fredrickson et al. 2001; Zachara et al. 2001; Peltier et al. 2003; Leermakers et al. 2005; Cooper et al. 2006). In the sulfidic zone, many trace metals, especially chacophiles like Pb, Zn, Cd or Cu, are often present in metal sulfide phases (Morse and Arakaki 1993; Huerta-Diaz et al. 1993, 1998; Rickard et al. 1995; Morse and Luther 1999). Changes in redox zonation can redistribute metals among the various aqueous and solid phases (Hamilton-Taylor and Davison 1995).

Macrophytes have the potential to change redox stratification and metal distribution through at least three distinct processes: (1) release of O_2 through roots into the rhizosphere, (2) primary production, increasing the quantity of labile organic carbon and (3) direct metal uptake into roots, rhizomes, stems and leaves. The release of O_2 into anoxic water-saturated soils or sediments at depth can create microzones of very different chemistry from the surrounding "bulk" geochemistry (Crowder 1991; Doyle and Otte 1997; Weis and Weis 2004). For example, Fe(III) oxide "plaques" can be formed in the rhizosphere as O_2 leaked from roots reacts with dissolved Fe(II) in surrounding bulk suboxic soils or sediments (Mendelssohn and Postek 1982; Crowder 1991; Ye et al. 1998a; Zhang et al. 1998; Batty et al. 2000, 2002; Weis and Weis 2004). These plaques may be important for sequestering nutrients, especially phosphorous, as well as trace elements (Crowder 1991; Ye et al. 1998a; Batty et al. 2000, 2002; Hansel et al. 2001). Macrophyte primary productivity produces organic matter than fuels aerobic and anaerobic respiration reactions, depleting terminal electron acceptors and creating more compressed redox zonation (Crowder 1991; Hines et al. 1989, 1999; Koretsky et al. 2005). Freshwater wetland macrophytes, such as *Typha* spp. (Crowder 1991; Ye et al. 1997; Demirezen and Aksoy 2004), *Phragmites* spp. (Crowder 1991; Keller et al. 1998; Ye et al. 1998a, b; Batty et al. 2000; Weis and Weis 2004), *Scirpus* spp. (Bhattacharya et al. 2006) and *Lemna* spp. (Zayed et al. 1998; Mkandawire et al. 2004; Oporto et al. 2006; Sweidan and Fayyad 2006) can uptake metals, concentrating them in both aboveground and belowground biomass. Macrophytes also have a significant influence on pore water and solid phase chemistry via nutrient uptake and release (through decaying litter) and evapotranspiration (Hines et al. 1989, 1999; Weis and Weis 2004; Choi et al. 2006; Kaldy et al. 2006).

Macrophyte densities and species can vary significantly, even over small areas within wetlands, which could lead to significant lateral variability in soil or sediment biogeochemistry. Most detailed studies of wetland geochemistry that have considered lateral heterogeneity have focused on only a few parameters (e.g. nutrient, trace metal or carbon geochemistry). There is a paucity of freshwater wetland studies, particularly for minerotrophic fens, with suites of data including trace metal distribution profiles together with profiles of nutrients, major elements and redox-sensitive species (e.g. pH, alkalinity, dissolved Fe(II), Fe(III), Mn(II), sulfide and sulfate) from adjacent sites with differing densities and types of vegetation.

In this study, pore water and solid phase geochemistry was studied at four sites in a minerotrophic fen. Pore waters from the upper 50 cm of each site were analyzed for a suite of nutrients, major and minor elements and redox sensitive species at 1–2 cm vertical resolution. Sequential sediment extractions were used to determine the partitioning of trace metals among four operationally defined solid phases as a function of depth. The four sites were located within a relatively small area of the marsh ($\sim 10\ m^2$), nonetheless, each site contained distinct types and densities of vegetation, suggesting that lateral heterogeneity might be significant. The study sites were also chosen to coincide with the site of a detailed seasonal study completed in this same marsh during 2002 (Koretsky et al. 2006a). Thus, differences in marsh geochemistry arising from changes in vegetation and interannual variations in local climate could also be assessed.

Field site

Kleinstuck Marsh is a minerotrophic fen located within a ~ 50 acre preserve in an urbanized area of Kalamazoo County, in southwestern Michigan (Buechler 1996; Koretsky et al. 2006a). The fen area

is glacial in origin with underlying gravel and sand glaciofluvial sediments typical of the region (Buechler 1996). The study area is presently recharged primarily by groundwater with some additional input of surface water runoff and precipitation, although in the past, the area may have been a precipitation-fed bog. Logging and peat mining in the 19th and early 20th century probably transformed the area from a bog into a fen with significant connection to the local groundwater (Buechler 1996).

The area of the fen chosen for study here was also the subject of a seasonal study of marsh geochemistry completed in 2001–2002 (Koretsky et al. 2006a). That study demonstrated that the upper layers of the peat are organic rich (35–50% organic carbon), strongly redox stratified and that the stratification changes significantly with season. The upper 50 cm are comprised of hemist soils (mucky peat), with plant fibers mostly decomposed. Four sites, located at the corners of an $\sim$10 m^2 area, were chosen for study here. These sites are located with $\sim$10–20 m of the sites used in the study of Koretsky et al. (2006a). There are striking differences in the appearance of the marsh in summer 2002 compared to summer 2006. In the present study, completed in July and August 2006, the marsh is visually much drier than during 2002 with no standing water at the marsh surface, except immediately following precipitation events. However, all four sites did appear to be completely saturated during peeper placement and removal (see below), with no apparent drying of the uppermost peat layers. In comparison, during summer 2002, $\sim$30 cm of standing water covered the peat surface in this area of the marsh. Much denser vegetation is also present compared to summer 2002. In particular, during summer 2006 the density of narrow-leaf cattails (*Typha angustifolia*) was considerably greater than in summer 2002. Also notable was the presence of the invasive purple loosestrife (*Lythrum salicaria*), which was not present in 2002. The most abundant vegetation types within a 1 m^2 area surrounding each of the four sites used for pore water and solid phase sampling in this study are listed in Table 1. Although these sites were all located within an $\sim$10 m^2 area, it is clear that there is considerable heterogeneity in vegetation types and densities. Peat surface temperatures (measured when peepers were removed) averaged 21°C.

Materials and methods

Pore water sampling and analyses

Pore waters were collected anaerobically at 1–2 cm intervals from the surface to a depth of $\sim$50 cm using acid-washed nylon dialysis equilibrators ("peepers"). Peepers were constructed in deionized water ($\geq$17.5 MΩ) using 0.2 μm pore size dialysis membranes, and were kept in water tanks deaerated with N_2 gas for at least 8 h prior to deployment in the field sites. Peepers were transported to the field in portable vinyl glove bags under positive N_2 pressure. At the field site, peepers were removed from the glove bags, immediately inserted into the peat and were left to equilibrate with the surrounding pore waters for $\sim$3 weeks. Peepers were then pulled from the peat, immediately inserted into a continuously N_2-flushed vinyl glove bag and transported back to the laboratory for sampling and analysis. Sampling was typically initiated less than 1 h after the initial removal of the peepers from the peat.

Pore waters were removed from the peeper chambers using disposable plastic syringes with stainless steel needles. The needles were used to puncture both the vinyl glove bag, which remained under positive N_2 pressure throughout the sampling, and the dialysis membrane covering a given chamber. The fluid was extracted from the chamber and filtered through a 0.2 μm nylon syringe filter. pH was measured on each sample and then the sample was divided among prepared vials for colorimetric analysis of alkalinity and dissolved Fe(II)/Fe(III), ΣPO_4^{-3}, ΣNH_3, ΣS^{-2}, Mn and SO_4^{-2} as described in Koretsky et al. (2003, 2006a, b). Remaining samples were preserved in trace metal grade nitric acid for analysis of major (Na, K, Mg, Ca) and trace (Co, Cr, Cu, Ni, Pb, Zn) elements by inductively coupled plasma optical emission spectroscopy (ICP-OES) on a PerkinElmer Optima 2100DV instrument. Prior to ICP-OES analyses, samples were diluted (as necessary) and spiked with an internal standard of 100 ppb In, Y, Bi, Ho and Sc.

Solid phase sampling and analyses

Peat cores were extracted using a Russian peat corer (Aquatic Research Instruments) to minimize compaction. Cores taken at each of the four sites were sectioned on site, under ambient atmosphere, into

Table 1 Vegetation at the four sampling sites

Vegetation	Site 1 (per m^2)	Site 2 (per m^2)	Site 3 (per m^2)	Site 4 (per m^2)
Purple Loosestrife (*Lythrum salicaria*)	0	0	1	0
Narrow Leaf Cattail (*Typha angustifolia*)	7	19	23	13
Bottlebrush Sedge (*Carex hystericina*)	0	0	1	0
Arrowhead (*Sagittaria* sp.)	0	8	5	2
Bulrush (*Scirpus* sp.)	0	5	11	8
Reed Canary Grass (*Phalaris aquatica*)	40	15	0	0
Duckweed (*Lemna* sp.)	0	0	0	50% cover

5 cm intervals from the surface to approximately 50 cm depth. Each section was immediately placed into a plastic baggie, which was sealed with as much air as possible squeezed out, returned to the laboratory and within 1 h of collection was placed into a Coy anaerobic chamber (85% N_2, 10% CO_2 and 5% H_2) for storage.

A sequential sediment extraction procedure, adapted from Tessier et al. (1979, 1982) was used to assess the partitioning of trace elements among four operationally defined, potentially labile fractions: exchangeable, carbonate, reducible and oxidizable. Briefly, approximately 1 g (exact weight recorded) of homogenized, freeze-dried peat was extracted using the reagents and procedures in Table 2. After mixing with each reagent for the specified period of time, the remaining solid phase was separated from the supernatant by centrifuging at 10,000 rpm for ~30 min. The supernatant was carefully removed, syringe-filtered and acidified with trace metal grade nitric acid prior to preparation (by appropriate dilution and addition of internal standard) for ICP-OES analyses. The remaining solid residue was then washed by adding 8 ml of deionized water, shaking for 15–20 min and then centrifuging at 10,000 rpm for 15–30 min. The wash supernatant was carefully removed from the remaining solids and discarded and the next sequential reagent was added to the remaining solid residue.

Organic carbon content was determined as a function of depth by measuring weight loss-on-ignition (LOI) at 550°C for 2 h (Heiri et al. 2001). Percent LOI was converted to percent organic carbon using the formula given by Craft et al. (1991):

$$\text{Organic C} = 9.40 \cdot \text{LOI} + 0.0025 \cdot \text{LOI} \cdot \text{LOI} \quad (1)$$

For one of the sites, the percentage organic carbon was also determined mannometrically (Krishnamurthy et al. 1999).

Results

Pore waters

pH profiles at the sites are very similar (Fig. 1A). pH decreases most sharply over the upper 10 cm from values between 7 and 8 at the surface, then declines more slowly to ~20 cm depth. From 20 cm to 50 cm depth, a constant pH of ~6.5 is observed at all four sites. Alkalinity increases with depth at all four sites,

Table 2 Sequential extraction procedures

Fraction	Reagent	Procedure
Exchangeable	8 ml 1 M $MgCl_2$, pH 7.0	1 h on shaker at room T
Carbonate	8 ml 1 M sodium acetate, pH 5.0 (adjusted with acetic acid)	5 h on shaker at room T
Reducible	20 ml of 0.04 M hydroxylamine HCl in 25% (v/v) acetic acid	6 h at 96°C in water bath, occasional agitation
Oxidizable	(1) 3 ml of 0.02 M HNO_3 + 5 ml 30% H_2O_2 (pH 2)	(1) 2 h at 96°C, occasional agitation; cool
	(2) 5 ml of 3.2 N ammonium acetate in 20% (v/v) HNO_3, dilute to 20 ml	(2) 30 min on shaker at room T

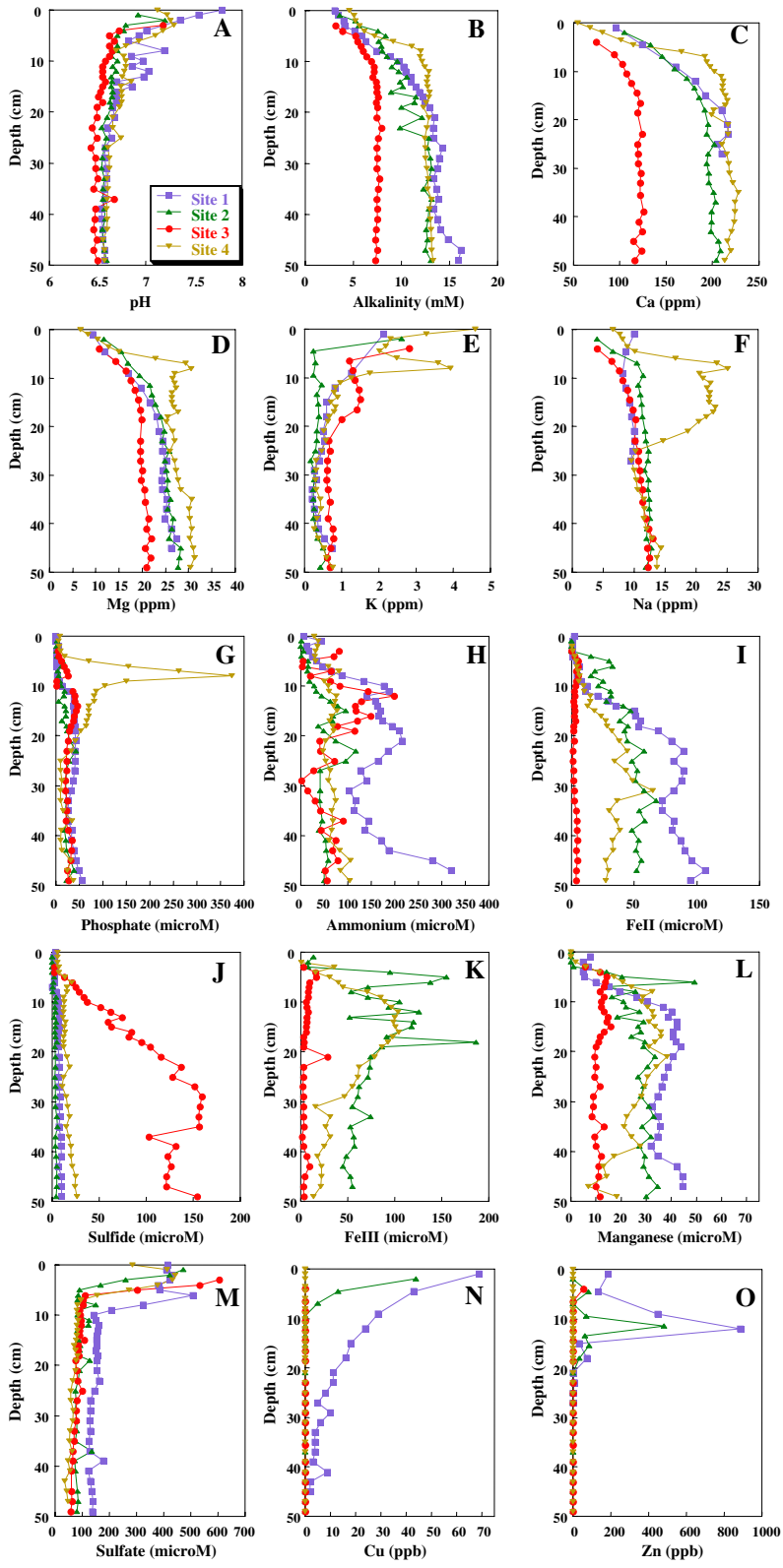

Fig. 1 Pore water geochemistry at the four sites as a function of depth over the upper 50 cm of peat: (**A**) pH, (**B**) alkalinity, (**C**) Ca, (**D**) Mg, (**E**) K, (**F**) Na, (**G**) total phosphate, (**H**) total ammonium, (**I**) Fe(II), (**J**) total sulfide, (**K**) Fe(III), (**L**) Mn, (**M**) sulfate, (**N**) Cu and (**O**) Zn. Dissolved Ca and Na were not measured below 28 cm depth at site 1

with a more rapid increase in the upper 10 cm of peat and essentially constant values from 20 cm to 50 cm depth at all four sites (Fig. 1B). Profiles at sites 1, 2 and 4 are similar, reaching levels of ~13 mM alkalinity by 20–25 cm depth. Alkalinity values at site 4 between 5 cm and 15 cm depth are slightly higher than at sites 1 and 2. Alkalinity profiles at site 3 are significantly different than at the other sites. At site 3, alkalinity increases much more slowly with depth, reaching a value of only ~7 mM.

Dissolved Ca profiles are similar in shape to those of alkalinity (Fig. 1C), with increasing concentrations from the surface to ~20 cm depth and then relatively little depth-dependence in the bottom half of the profile. Sites 1, 2 and 4 have similar values, except that higher Ca concentrations are present between 5 cm and 15 cm depth at site 4 compared to the other sites. Site 3 values are again much lower than at the other sites, reaching only ~115 ppm by 50 cm depth, compared to ~210 ppm by 50 cm depth at sites 2 and 4. Dissolved Mg concentrations also increase with depth (Fig. 1D). As for Ca and alkalinity, dissolved Mg levels are elevated at site 4 between ~5 cm and 20 cm of depth. Concentrations of Mg are lower at site 3 than at the other sites, although the difference is less pronounced than for Ca and alkalinity.

Dissolved K profiles have a markedly different depth-dependence compared to Mg and Ca (Fig. 1E). At all four sites, dissolved K decreases from 2 ppm to 5 ppm at the surface to ~0.5 ppm at 20 cm depth. K profiles are very similar at the four sites, with slightly more K present at site 4 and slightly less K at site 2 present between 5 cm and 10 cm depth compared to sites 1 and 3. Dissolved Na profiles at sites 1, 2 and 3 are very similar, increasing gradually with depth to ~12–13 ppm at 50 cm depth (Fig. 1F). In contrast, between 5 cm and 25 cm depth, site 4 has much higher Na concentrations compared to the other sites, with levels of up to 25 ppm.

Dissolved phosphate concentrations are typically 50 μM or less at all four sites and vary little with depth (Fig. 1G). The exception is at site 4, where there is a sharp peak in phosphate with a maximum of nearly ~375 μM centered at 8 cm depth. At all four sites, dissolved ammonium is much more variable with depth than phosphate (Fig. 1H). At sites 2, 3 and 4, dissolved ammonium levels are steady at ~50–100 μM from 20 cm to 50 cm depth. There is a small subsurface peak in ammonium at site 3 with a maximum of ~200 μm at 12 cm depth. In contrast to the other three sites, ammonium concentrations continue to build with depth to ~320 μM by 50 cm depth at site 1.

Dissolved Fe(II) concentrations are more variable between sites than nutrients or major elements (Fig. 1I). Dissolved Fe(II) is very low (<6 μM) throughout the upper 50 cm of peat at site 3. At sites 1, 2 and 4, Fe(II) increases with depth, with the highest Fe(II) concentrations at site 1 and the lowest at site 4. Dissolved sulfide profiles are similar at sites 1, 2 and 4 (Fig. 1J). At these sites, sulfide concentrations are low and increase only slightly with depth, with the greatest sulfide levels of the three sites occurring at site 4, which also had the lowest Fe(II) concentrations. As for Fe(II), the sulfide profile at site 3 is quite distinct from those measured at the other three sites. Sulfide concentrations increase dramatically with depth, reaching ~160 μM by ~30 cm depth.

Dissolved Fe(III) levels, like Fe(II), are much lower at site 3 than at the other sites (Fig. 1K). Fe(III) was not measured at site 1. At sites 2 and 4, Fe(III) profiles are quite similar with a broad maximum of 100–150 μM centered at ~15 cm depth. Dissolved Mn profiles are similar to dissolved Fe(II) profiles (Fig. 1L). Mn concentrations are much lower (~10–15 μM) and less variable at site 3 compared to the other sites. At sites 1, 2 and 4, Mn concentrations increase with depth to ~30 μM by ~10–15 cm depth. As for Fe(II), the highest dissolved Mn concentrations are measured at site 1.

Dissolved sulfate profiles are similar at the four sites (Fig. 1M). Concentrations are highest close to the surface, reaching ~450–600 μM, with the highest values at site 3 and the lowest at site 4. At all four sites, sulfate concentrations decrease rapidly over the upper 5 cm. At site 1, levels continue to decrease until 10 cm depth. Beneath the zone of rapid sulfate depletion, sulfate concentrations at sites 2, 3 and 4 decrease very gradually with depth, from ~100 μM to ~50 μM at the bottom of the profiles. Sulfate concentrations are also nearly invariant with depth at site 1, but are slightly higher than at the other three sites, averaging ~150 μM.

ICP-OES was used to analyze pore waters for Co, Cr, Cu, Ni, Pb, and Zn. Concentrations of Co, Cr, Ni and Pb were consistently below detection limits of ~10 ppb. Dissolved Cu concentrations were close to

detection limits of ~10 ppb throughout sites 3 and 4. At site 2, Cu concentrations reached ~44 ppb at 2 cm depth and decreased to below detection limits by a depth of 9 cm (Fig. 1N). Dissolved Zn concentrations were also close to detection limits at all depths at site 4, and only a small peak in Zn of ~50 ppb at 4 cm depth was present at site 3 (Fig. 1O). However, at both sites 1 and 2, a large peak in Zn reaching nearly 900 ppb at site 1 and nearly 500 ppb at site 2 is centered at 12 cm depth.

Tessier extractions

Metals associated with the operationally-defined readily exchangeable, carbonate, reducible and oxidizable fractions were assessed using the extraction scheme proposed by Tessier et al. (1979). The reducible fraction is commonly assumed to represent metals associated with iron and manganese oxides, and the oxidizable fraction is likely comprised of a mixture of metals associated with both organic matter and sulfides. Concentrations of Cd, As, Cr and Co were typically near or below detection limits of ≤ 1 μg/g dry soil (steps 1, 2 and 4) or ≤ 5 μg/g dry soil (step 3; higher detection limits due to greater dilution for analysis of supernatants in the organic-rich matrix). Distributions of Cd and As are not shown. Metals associated with the oxidizable fraction of site 2 were not analyzed due to a sampling error.

At all four sites, exchangeable and carbonate associated Fe accounts for very little (<1%) of the extracted Fe (Fig. 2). The reducible-Fe decreases significantly with depth at all sites, with the largest decrease and lowest concentrations of reducible-Fe occurring at site 3, and the largest concentrations of reducible-Fe in the upper portion of the peat profile occurring at site 1. Oxidizable-Fe dominates the distribution of Fe at all three sites where this fraction was analyzed. At site 1, there is more oxidizable-Fe at the bottom of the core, in contrast to site 3, which has the highest oxidizable-Fe concentrations in the upper 5–30 cm.

The distribution and total quantity of extracted Mn is similar at the four sites, although there is a little less Mn present in the sum of the labile solid fractions at Site 3 compared to the other sites (Fig. 3). In contrast to Fe, a significant quantity of Mn is associated with all four operationally-defined fractions. There is more exchangeable-Mn present at site 4 compared to the other three sites. Especially at sites 2 and 4, carbonate-associated Mn decreases markedly with depth. At all four sites, the quantity of Mn associated with the reducible fraction also decreases with depth. At site 3, there is less reducible-Mn present in the upper 20 cm of the peat than at the other three sites, but the quantity below 35–40 cm is similar at all four sites. Mn associated with the oxidizable fraction varies little with depth and typically accounts for ~15–20% of the extracted Mn.

Most of the extracted Ba is associated with the reducible and exchangeable fractions, although a significant quantity is also associated with the carbonate and oxidizable fractions (Fig. 4). The quantity of exchangeable-associated Ba generally increases with depth and is highest at sites 3 and 4. Less Ba is extracted with the carbonate phase at site 3 compared to the other sites. At site 3, carbonate-Ba increases at the bottom of the core, in contrast to the other sites where carbonate-Ba decreases with depth. Site 3 also has the smallest quantity of reducible-Ba. At sites 1, 2 and 4 reducible-Ba decreases with depth, whereas the reducible-Ba at site 3 varies little with depth, resulting in similar concentrations of reducible-Ba at the bottom of all four cores. Oxidizable-Ba concentrations are similar at sites 1, 3 and 4, typically accounting for 15–25% of total extracted Ba.

The extracted Ni distribution is similar at the four sites (Fig. 5). At all sites, exchangeable-Ni accounts for a negligible (<1%) fraction of extracted Ni and carbonate-associated Ni typically accounts for <5% of extracted Ni. Ni extracted with the reducible fraction usually accounts for 15–25% of total extracted Ni. Ni associated with this fraction decreases with depth at all four sites. The smallest concentrations of reducible-associated Ni, especially at the top of the peat profile, occur at site 3. Oxidizable-Ni dominates the distribution of Ni. The concentration of Ni in this fraction varies little with depth at sites 1 and 4, and decreases with depth only in the lower 15 cm at site 3.

Most of the extracted Zn is associated with either the oxidizable or reducible fractions (Fig. 6). The reducible-associated Zn decreases with depth at sites 1, 2 and 3, which all have very similar concentrations of reducible-Zn, except in the upper 5 cm of the peat profile, where there is more Zn associated with the reducible phase at site 2 compared to the other sites.

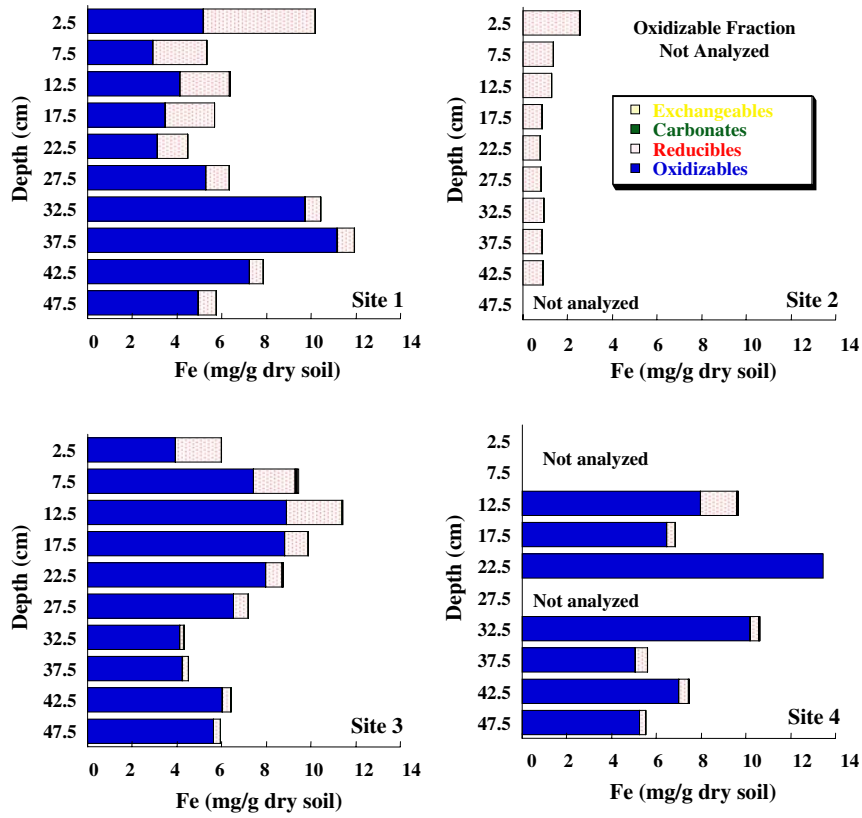

Fig. 2 Distribution of Fe among the four operationally defined solid phase fractions (exchangeable, carbonate, reducible and oxidizable) as a function of depth at each of the four sites

Oxidizable-associated Zn increases gently with depth at site 1, which also typically has the lowest concentrations of oxidizable Zn. Site 3 has the highest concentrations of oxidizable Zn, and in contrast to site 1, oxidizable-Zn quantities are greatest in the shallower samples. At site 4, oxidizable-Zn levels are typically intermediate between those measured at sites 1 and 3, and as for site 1, increase with depth.

Nearly all extracted Pb is associated with the oxidizable fraction, with a small quantity of Pb extracted with the carbonate fraction (Fig. 7). The oxidizable-Pb profiles at the different sites are quite distinct. At site 1, the oxidizable Pb fraction decreases from ~20 μg Pb/g dry soil in the upper 5 cm to just ~3 μg Pb/g dry soil at 15–20 depth, and then increases dramatically below 30 cm depth to levels as high as 35 μg Pb/g dry soil. In sharp contrast, at site 3, most of the oxidizable-Pb is extracted in the upper portion of the core. At this site, oxidizable-Pb levels increase from 30 μg Pb/g dry soil in the upper 5 cm to a maximum of 54 μg Pb/g dry soil at 15–20 cm depth and then decrease to just 4.5 μg Pb/dry soil at 45–50 cm depth. The depth distribution of oxidizable-Pb at site 4 is intermediate between those at sites 1 and 3, with maximum levels of Pb extracted between ~25 and 35 cm depth.

As for Pb, the bulk of the extracted Cu is associated with the oxidizable fraction (Fig. 8). There is relatively little variation in oxidizable-Cu with depth at sites 1 and 4. In contrast, at site 3 the concentration of oxidizable-Cu decreases below 15–20 cm depths, with much lower concentrations present below 35 cm depth compared to the upper portion of the profile. A small amount of Cu (typically <2 μg Cu/g dry soil), relatively invariant with depth or site, is associated with the reducible fraction. These levels are very close to the detection limits for this extraction step.

At all four sites, extractable Co levels are very low, with concentrations only above detection limits in the oxidizable fraction (Fig. 9). The depth distributions of oxidizable-Co at the four sites are muted versions of those observed for Pb and Cu. At site 1,

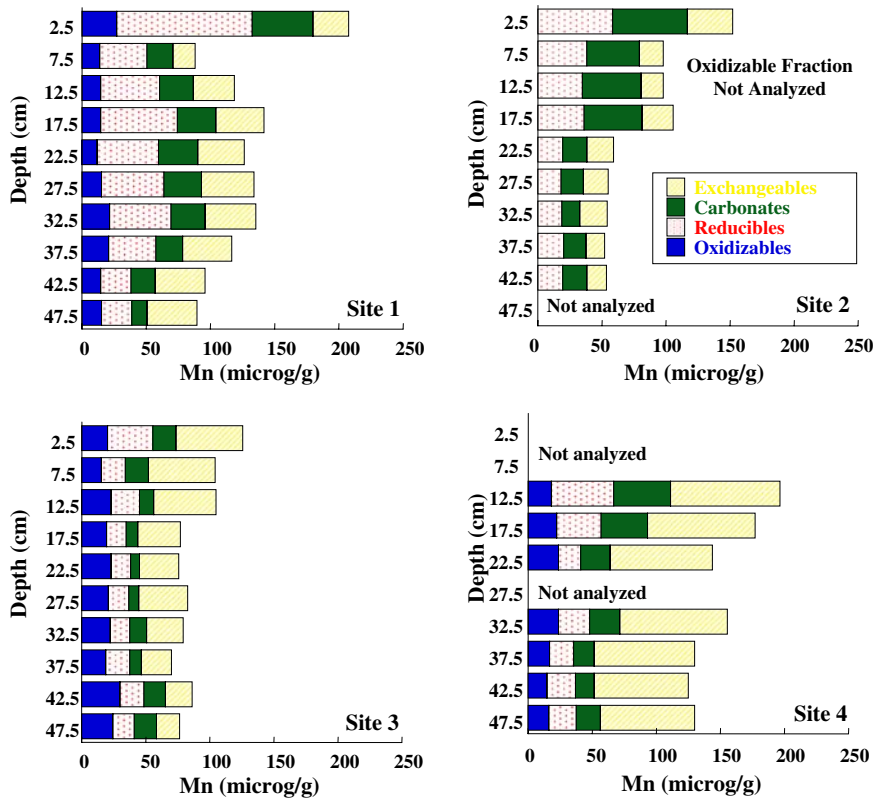

Fig. 3 Distribution of Mn among the four operationally defined solid phase fractions as a function of depth at each of the four sites

oxidizable-Co increases gradually with depth, whereas at site 3, maximum concentrations occur between 10 cm and 25 cm depth.

Extractable Cr concentrations are close to detection limits. Most of the Cr is associated with the oxidizable fraction (Fig. 10). The depth distribution of oxidizable-Cr is very similar to the depth distributions of oxidizable Co, Pb and Cu. The small quantity of Cr extracted in the reducible fraction (~2–3 μg Cr/g dry weight soil) is close to the detection limits, and varies little with depth or site.

Percent organic carbon

Percent organic carbon determined by LOI is similar at the four sites. At all four sites, the percent organic carbon decreases from ~45% near the peat surface to ~25% at ~45 cm depth (Fig. 11). In the 45–50 cm interval, there is more divergence in the percent organic carbon values, from ~12% at site 3 to ~32% at site 4. For samples from site 3, percent organic carbon was also analyzed using a mannometric technique (data courtesy of Drs. RV Krishnamurthy and Tsigabu Gebrehiwet, WMU Geosciences). There is excellent agreement between these data and the percent organic carbon estimated from LOI according to the method of Craft et al. (1991).

Discussion

Redox stratification

Wetland soils or sediments are typically vertically redox-stratified, with progressively more reducing conditions found with increasing depth. As described above, oxic, suboxic, sulfidic and methanic zones have been delineated based on pore water profiles of Mn(II), Fe(II) and sulfide for saltmarshes (e.g. Koretsky et al. 2003, 2005; CM Koretsky et al. submitted), lake sediments (e.g. Koretsky et al. 2006b) and minerotrophic fens (e.g., Koretsky et al. 2006a). The oxic zone is defined by the presence of dissolved oxygen and is generally very

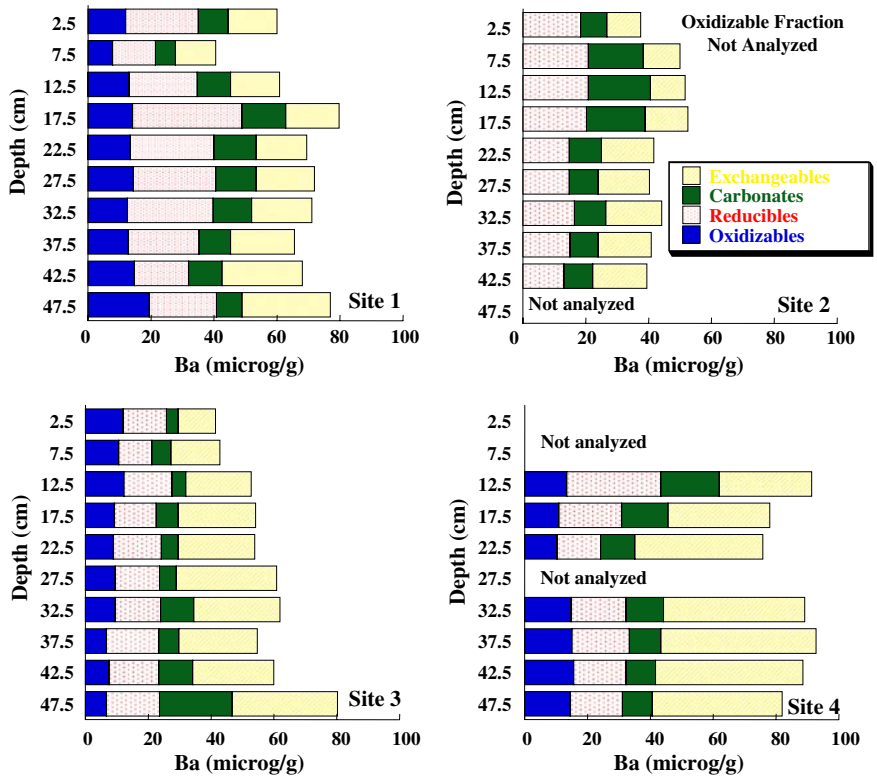

Fig. 4 Distribution of Ba among the four operationally defined solid phase fractions as a function of depth at each of the four sites

thin in organic-rich sediments or soils. Within this zone, organic matter degradation is presumed to occur primarily aerobically. Dissolved species such as Mn(II), Fe(II) or sulfide diffusing upwards from more reduced deeper layers can be oxidized within the oxic zone by oxygen. The suboxic zone is identified in this study, as in previous studies, based on the accumulation of dissolved Mn(II) and Fe(II) in the pore waters, products of anaerobic reductive dissolution of Mn(IV) and Fe(III) oxides. In the sulfidic zone dissolved sulfide builds up in the pore waters due to anaerobic sulfate reduction. Once sulfate is depleted to concentrations limiting microbial respiration, organic matter degradation occurs predominantly via methanogenesis. The vertical sequence of zonation is often attributed to differences in the energetic favorability of coupling the various terminal electron acceptors (O_2, Mn(IV), Fe(III), sulfate) to organic matter oxidation (e.g., Froelich et al. 1979). However, it is important to note that in laterally heterogeneous, organic-rich soils or sediments, it is likely that organic matter degradation occurs by more than one pathway within each of the pore water zones. For example, rhizosphere oxygen leakage into a bulk suboxic or sulfidic zone creates oxic microzones (Crowder 1991; Pedersen et al. 1998; Jensen et al. 2005; Choi et al. 2006), supporting aerobic respiration and increasing microbial Fe(III) reduction (Roden and Wetzel 1996). Pore water redox stratification at the Kleinstuck marsh is strongly dependent on season (Koretsky et al. 2006a), and is likely to depend on densities and types of vegetation (e.g. Jaynes and Carpenter 1986).

All four sites have very similar pH profiles with a fairly rapid decrease in pH occurring in the upper 5 cm of the peat profile (Fig. 1A). The increased acidity is likely produced by oxygen oxidizing organic matter and dissolved inorganic species (e.g., Mn(II), Fe(II), NH_3) diffusing upwards from the more reduced, deeper layers. pH minima have sometimes been used to infer maximum oxygen penetration depths in organic-rich soils or sediments (Shotyk 1988; Koretsky et al. 2005, 2006a, b; CM Koretsky et al. submitted). However, the gentler decline in pH between 5 cm and 20 cm depth is probably not due to deep penetration of oxygen, although some oxygen may be introduced at these depths by rhizosphere

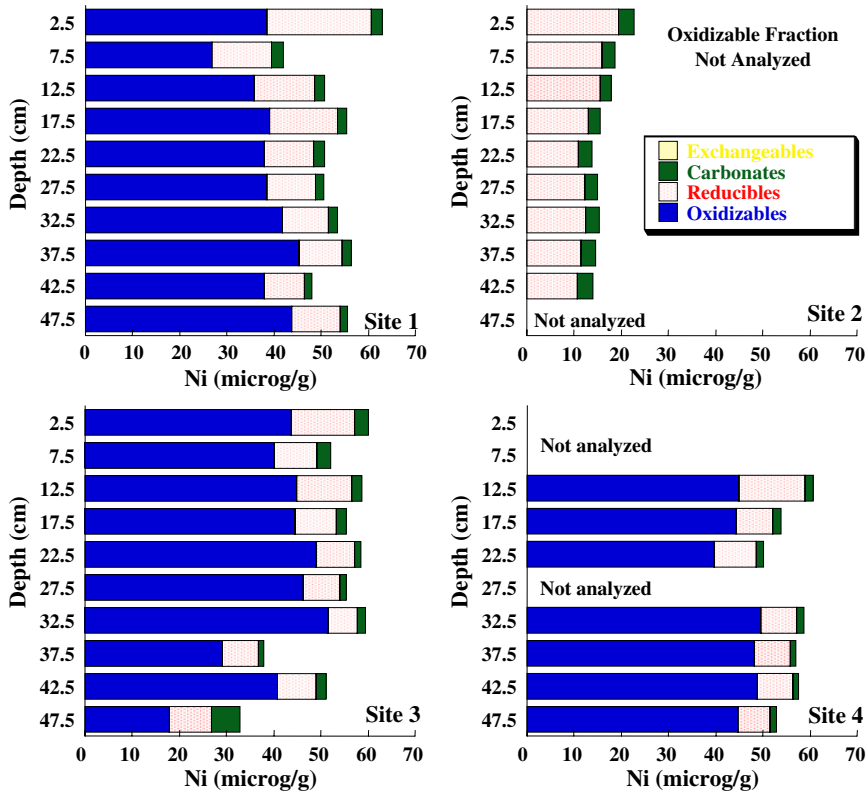

Fig. 5 Distribution of Ni among the four operationally defined solid phase fractions as a function of depth at each of the four sites

oxygen leakage. Instead, this decline in pH is more likely due to precipitation of carbonate phases, according to

$$Ca^{+2}_{(aq)} + HCO^{-}_{3\,(aq)} = CaCO_{3(s)} + H^{+}_{(aq)}, \quad (2)$$

which produces acidity (see also Major elements section).

Total alkalinity at these sites is dominated by carbonate alkalinity (Koretsky et al. 2006a). Alkalinity profiles are thus likely to represent the balance of alkalinity production from anaerobic degradation of organic matter and carbonate dissolution and removal of alkalinity via carbonate precipitation reactions. The rapid accumulation of alkalinity in the upper 10 cm of the peat (Fig. 1B) suggests high rates of organic matter decay in the uppermost portion of the peat profile, which is also supported by the decreasing percent organic carbon with depth at all four sites (Fig. 11). At three of the sites, the alkalinity profiles are quite similar, but there is a distinctly smaller accumulation of alkalinity at site 3. There are several possible explanations for this, including: (1) less primary production, and thus less organic matter degradation, at site 3, (2) similar primary production, but lower rates of organic matter degradation at site 3, (3) more removal of bicarbonate into the carbonate solid phase at site 3, or (4) differences in the dominant organic matter degradation pathway at site 3 compared to the other sites.

The amount of alkalinity produced per mol of organic carbon oxidized depends on the reaction pathway (Van Cappellen and Wang 1996). Specifically, anaerobic respiration of organic matter via dissimilatory manganese reduction produces 4 moles of alkalinity per mol organic C, according to:

$$CH_2O_{(aq)} + 2MnO_{2(s)} + 3CO_{2(aq)} + H_2O_{(l)} = 2Mn^{+2}_{(aq)} + 4HCO^{-}_{3\,(aq)} \quad (3)$$

while dissimilatory iron reduction produces 8 moles of alkalinity per mole of organic C oxidized,

$$CH_2O_{(aq)} + 4Fe(OH)_{3(s)} + 7CO_{2(aq)} = 4Fe^{+2}_{(aq)} + 3H_2O_{(l)} + 8HCO^{-}_{3\,(aq)} \quad (4)$$

and microbial sulfate reduction produces only 1 mol of alkalinity per mol of organic C oxidized,

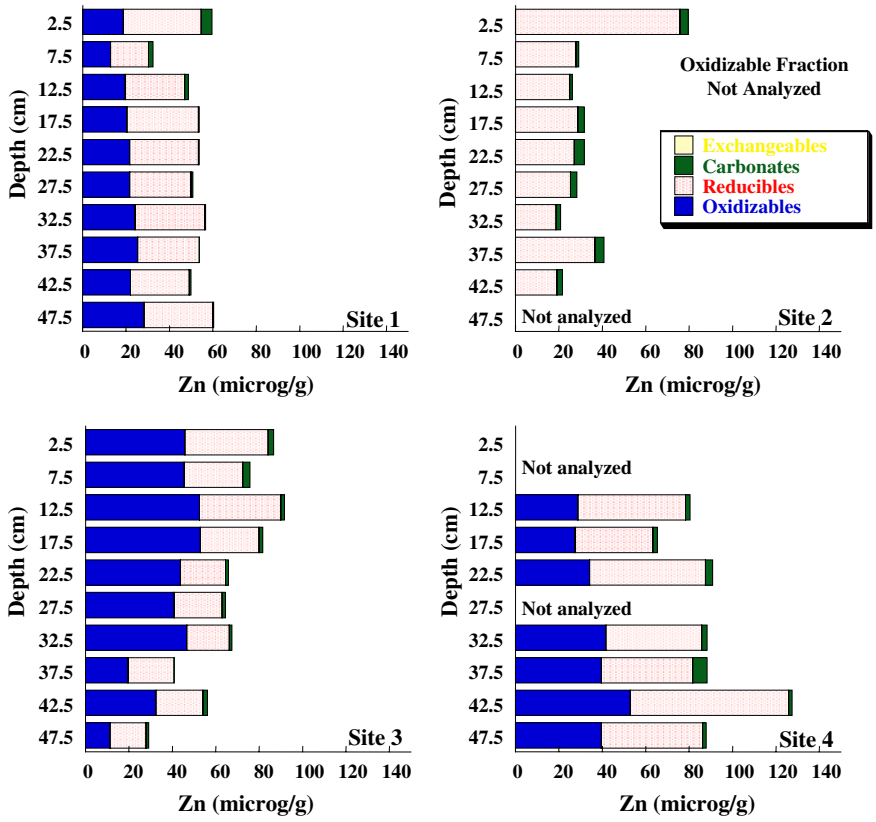

Fig. 6 Distribution of Zn among the four operationally defined solid phase fractions as a function of depth at each of the four sites

$$CH_2O_{(aq)} + 1/2SO^{-2}_{4\,(aq)} = 1/2H_2S_{(aq)} + HCO^{-}_{3\,(aq)}. \quad (5)$$

Without direct measurements of primary productivity or organic matter respiration rates at the sites, it is difficult to assess the first and second possible explanations for the lower alkalinity accumulation at site 3, although the similarity of the percent organic carbon profiles with depth at the four sites (Fig. 11) argues against these hypotheses. Common carbonate minerals are consistently undersaturated at site 3 (see Major elements section), so excess carbonate precipitation at site 3 compared to the other sites is unlikely to account for the lower measured alkalinities. However, organic matter respiration pathways inferred from the bulk redox stratification at the four sites do point to a very different predominant organic matter pathway near the surface at site 3 compared to the other three sites.

Sites 1, 2 and 4 all have a large suboxic zone, with dissolved Mn(II) and Fe(II) accumulation beginning at depths of ~2 and 4 cm, respectively (Figs. 1I, L), Broad Mn(II) and Fe(II) peaks dominate the entire upper 50 cm at these three sites. There is also very little accumulation of sulfide at these sites (Fig. 1J). In sharp contrast, at site 3 dissolved Mn(II) concentrations in the pore waters are much lower compared to the other sites, there is very little dissolved Fe(II) present at any depth and dissolved sulfide increases rapidly with depth. These data suggest that either more organic matter degradation via sulfate reduction occurs at site 3 compared to sites 1, 2 and 4, or that sulfate reduction is not as closely balanced with sulfide oxidation at site 3. A close balance between sulfate reduction and sulfide oxidation has been observed in other wetland systems. For example, Wieder and Lang (1988) measured sulfate reduction rates in an acidic bog, and found very high rates of sulfate reduction, comparable to those in coastal marine sediments, in sediments with low bulk concentrations of sulfate (<200 μM). They suggested that the high sulfate reduction rates were supported by rapid sulfide oxidation. Urban et al. (1989), Wieder et al. (1990) and Blodau et al. (2007) similarly found rapid internal sulfur cycling, even

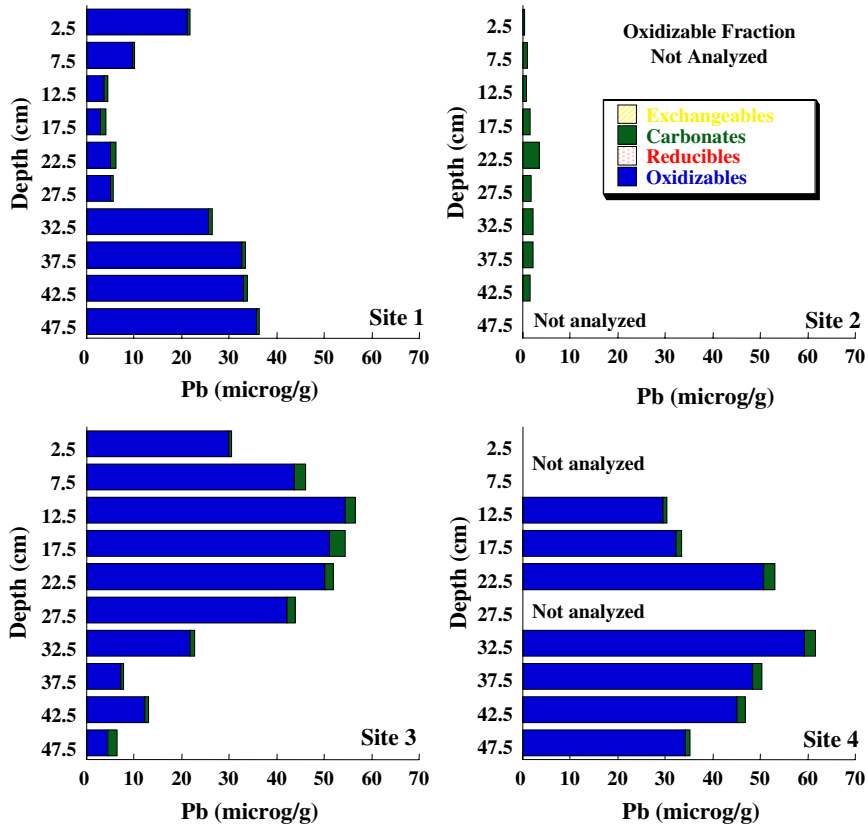

Fig. 7 Distribution of Pb among the four operationally defined solid phase fractions as a function of depth at each of the four sites

in the presence of low sulfate concentrations, in ombrotrophic bogs.

The distribution of Fe in the solid phase supports the hypothesis that more net sulfate reduction occurs at site 3 compared to the other sites. Site 3 has the lowest concentrations of reducible-associated Fe of the four sites and also has the highest levels of oxidizable-associated Fe in the upper portion of the peat (Fig. 2). This is consistent with consumption of readily reducible Fe(III) oxides, producing Fe(II) sulfides. Site 3 also has the lowest concentrations of reducible-associated Mn, again, suggesting that labile Mn(IV) oxides are depleted in a thin suboxic zone near the surface.

Interestingly, dissolved sulfate concentrations are quite similar at all four sites (Fig. 1M), in spite of the significant differences in dissolved sulfide concentrations and inferred differences in the proportion of organic matter degradation coupled to sulfate reduction. However, as indicated above, total concentrations of sulfate or sulfate profiles are often poor indicators of sulfate reduction rates due to rapid internal cycling of sulfur in wetlands (Berner 1980; Wieder and Lang 1988; Urban et al. 1989; Wieder et al. 1990; Koretsky et al. 2005, 2006a). Sulfide diffusing upward into the oxic surface layer or into oxic microzones in the rhizosphere can be rapidly reoxidized to produce dissolved sulfate, obscuring the magnitude of sulfate reduction. Thus, without direct measurement of sulfate reduction rates, it is impossible to quantify the relative contribution of sulfate reduction to organic matter degradation at the four sites.

Given the close proximity of these sites (only ~2 m separates Sites 3 and 4), the substantial differences in pore water and solid phase biogeochemistry are remarkable. The sites do differ with respect to the type and density of vegetation (Table 1). The presence of purple loosestrife at site 3, lacking at the other three sites, is the most visually striking distinction. Site 3 also contains bottlebrush sedge, which is not present at the other three sites, and it has the highest density of cattails and bulrush of the three sites. These results highlight the potential for very

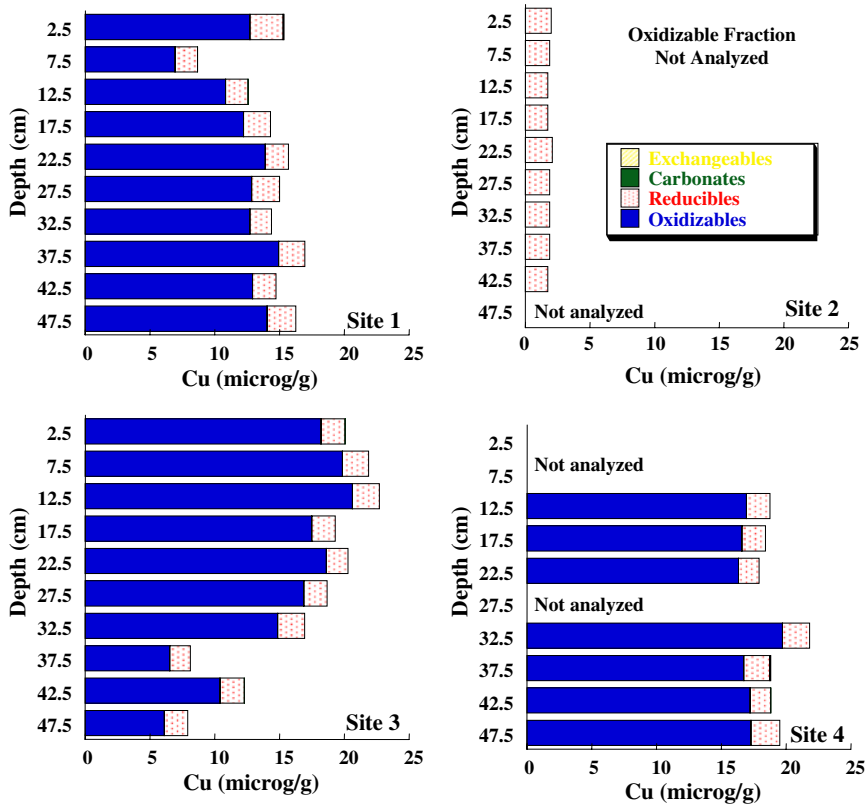

Fig. 8 Distribution of Cu among the four operationally defined solid phase fractions as a function of depth at each of the four sites

significant lateral heterogeneity of biogeochemical conditions in marshes, even over relatively small scales. These data also suggest that the exotic invasive purple loosestrife may create significant shifts in peat biogeochemistry.

Nutrients

Organic matter degradation releases dissolved phosphorous and nitrogen to pore waters (Mitsch and Gosselink 2000). Dissolved phosphate can be removed from the pore waters via adsorption onto particulates, precipitation of phosphate-bearing minerals or by macrophyte uptake. Low concentrations of phosphate are common in wetland pore waters, where macrophytes are frequently phosphate-limited. All four sites in this study have relatively low concentrations of phosphate (typically <50 μM), with the exception of a large peak in phosphate centered at ~8 cm at site 4 (Fig. 1G). This large peak in phosphate may indicate a localized area of high organic matter degradation, although levels of dissolved ammonium are not correspondingly higher at this depth at site 4 compared to the other sites. Major element data (see Major elements section) indicate enhanced evapotranspiration at site 4 in the upper portion of the peat relative to the other sites and this may contribute toward the observed subsurface peak in dissolved phosphate. Another possibility is that the phosphate is liberated from reductively dissolving Fe oxides. However, it is not clear why a similar peak is not observed at the other sites, unless the vegetation at those sites is more efficient at taking up any released phosphate. The peak in dissolved phosphate could also be due to differences in vegetation at the sites, either due to differential release of phosphate from various types of decaying plant matter, or, due to differential uptake of phosphate from the pore waters by the various plant species.

Dissolved phosphate concentrations may be controlled, at least in part, by precipitation of P-bearing minerals, such as strengite ($FePO_4 \cdot 2H_2O$) or hydroxylapatite ($Ca_5(PO_4)_3OH$). The saturation indices at each site as a function of depth for these two minerals were calculated using the speciation code JCHESS with the default thermodynamic database (van der

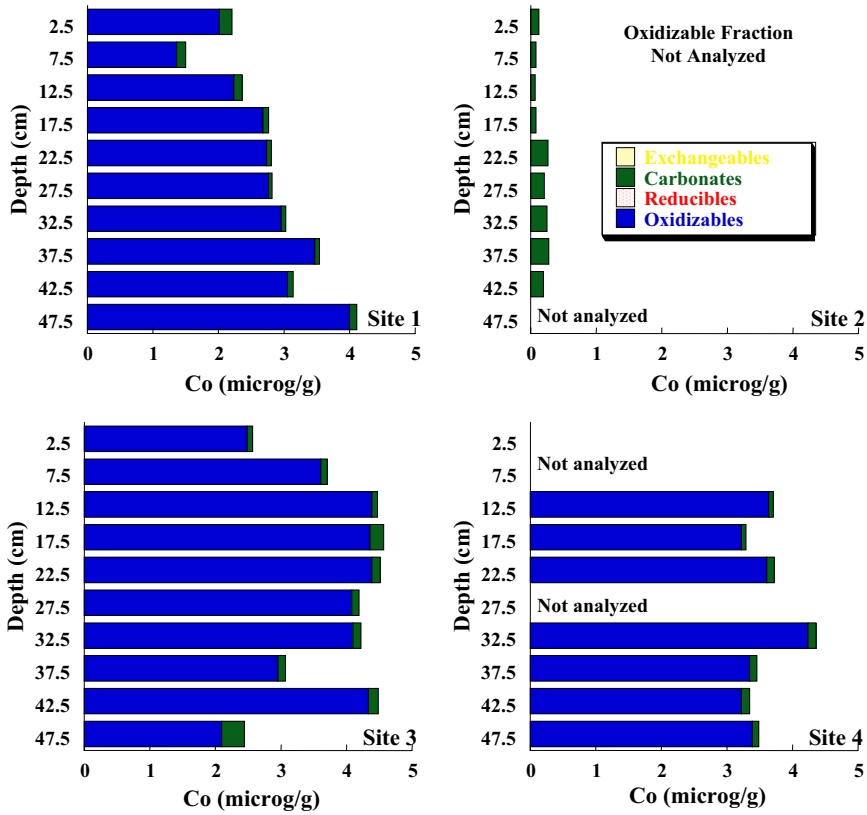

Fig. 9 Distribution of Co among the four operationally defined solid phase fractions as a function of depth at each of the four sites

Lee and de Windt 2000; Table 3). Speciation calculations were completed for the closed system by assuming that the measured alkalinity is equal to total $HCO^{-}_{3\,(aq)}$, and including the concentrations of all measured species in the calculations. The temperature for all speciation calculations was set to 25°C, because temperature profiles were not measured at the sites, and this is reasonably close to the measured surface temperature of the peat (~21°C) and the average air temperatures for July 2006 of 23°C reported at the nearby Kalamazoo airport (Wunderground 2007). Negative saturation indices indicate that the mineral is undersaturated; positive saturation indices indicate supersaturation. Except very near the surface, strengite is close to saturation at site 2, and is slightly undersaturated throughout site 3 (Fig. 12A). At site 4, strengite fluctuates between oversaturation (5–25 cm depth) and undersaturation (upper 5 cm and below 25 cm depth). Hydroxylapatite is similarly close to saturation at site 2 and undersaturated at site 3 (Fig. 12B). At site 1, hydroxylapatite is undersaturated in the upper 10 cm, but reaches near saturation at 25 cm depth. At site 4, hydroxylapatite is significantly oversaturated in the upper 25 cm, but remains close to saturation below 25 cm depth. These calculations suggests that precipitation of phases such as strengite or hydroxylapatite play a significant role in determining pore water concentrations of phosphate in these fen soils.

Dissolved ammonium released to the pore waters via organic matter degradation can be removed via macrophyte uptake, oxidation to form dissolved nitrite or nitrate or by sorption, especially onto clay minerals. Dissolved ammonium profiles are somewhat noisy, but generally suggest rapid accumulation of ammonium in the upper 10–15 cm of the peat with steady or slightly decreasing levels lower in the peat (Fig. 1H). The rapid accumulation of ammonium in the upper portion of the peat is probably due to higher organic matter degradation rates near the surface. Alkalinity, Fe(II) and Mn(II) levels are higher at site 1 than at sites 2 or 4, thus, the higher ammonium concentrations there may be due to higher organic matter degradation rates. It is also possible that

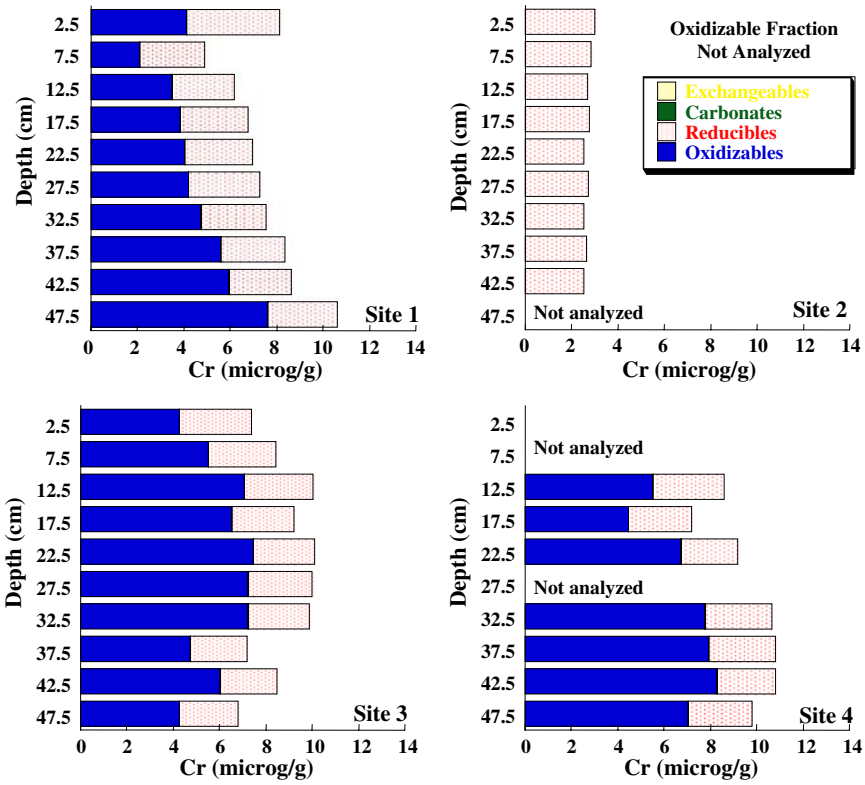

Fig. 10 Distribution of Cr among the four operationally defined solid phase fractions as a function of depth at each of the four sites

differences in rhizosphere oxygen leakage, and subsequent reoxidation of reduced species including ammonium, Mn(II) and Fe(II), or differences in direct uptake of dissolved ammonium by the macrophytes at site 1 contribute to the observed higher levels of ammonium. At site 1, there is a second accumulation of ammonium at depths below 30 cm. The increase corresponds to elevated dissolved Fe(II), and to a lesser extent, dissolved Mn(II). This "double" peak of Fe(II), Mn(II) and ammonium may be due to non-steady state effects as redox stratification undergoes seasonal shifts (Koretsky et al. 2006a). Alternatively, these peaks may indicate a zone of enhanced Fe(III) and Mn(IV) reduction at depth, perhaps corresponding to a region with elevated leakage of labile organic matter from deep macrophyte roots or with significant decay of senescent roots.

Dissolved trace metals

Concentrations of dissolved Co, Cr, Ni and Pb are always below the detection limit of ~10 ppb. However, at sites 1 and 2, high levels of Cu are detected near the surface, declining with depth (Fig. 1N). Cu can be released into solution by reductive dissolution of FMO or, more often, by degradation of organic matter or release of organic matter bound to dissolving FMO (Tessier et al. 1996; Achterberg et al. 1997). Although Fe(III) and Mn(IV) reduction are also inferred to occur in the upper portion of site 4, Cu does not accumulate in the pore waters at this site. This may reflect variability in macrophyte uptake of Cu due to the heterogeneous distribution of vegetation. For example, site 4 is the only site with duckweed, a plant that has been documented to accumulate Cu from pore waters (Zayed et al. 1998; Sweidan and Fayyad 2006). At site 3, any dissolved Cu produced by organic matter degradation or reductive dissolution of FMO is likely to be removed from the pore waters not only by organic matter association or macrophyte uptake, but also by forming discrete Cu sulfide minerals or associating with precipitating iron sulfides (Balistrieri et al. 1992b; Huerta-Diaz et al. 1993; Achterberg et al. 1997; Morse and Luther 1999; see also Solid phase metal distributions section).

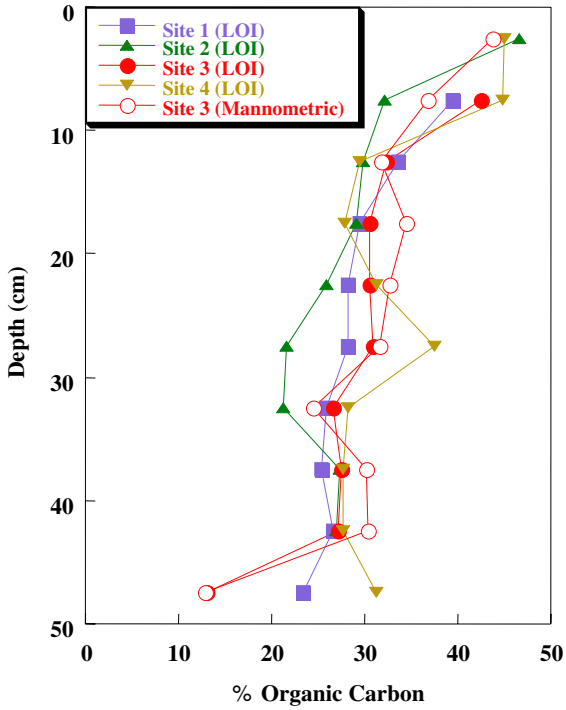

Fig. 11 Percent organic carbon as a function of depth at the four sites, determined by loss on ignition (closed symbols). At site 3, percent organic carbon was also determined mannometrically (open symbols)

Peaks in dissolved Zn occur between 5 cm and 15 cm depth at sites 1 and 2 (Fig. 1O). Reductive dissolution of FMO can release adsorbed or coprecipitated Zn into the pore waters, where it can be taken up by macrophytes (e.g. Ye et al. 1998b; Peltier et al. 2003; Bhattacharya et al. 2006), associated with organic matter or precipitated out in discrete Zn sulfide phases (Achterberg et al. 1997; Huerta-Diaz et al. 1998; Morse and Luther 1999; Peltier et al. 2003). Tessier extractions point to a large decrease in reducible-associated Zn between the upper 5 cm and 5–10 cm depth at both site 1 and 2 (Fig. 6), consistent with release of Zn associated with reductively dissolving FMO in the upper part of the suboxic zone. Zn is likely removed from the pore waters both via precipitation of sulfides and by macrophyte uptake, and possibly by complexation to solid phase organic matter. As for Cu, Zn is below detection limits at site 4, suggesting that uptake by vegetation at this site may limit the accumulation of Zn in the pore waters. For example, duckweed has also been shown to accumulate Zn (Sweidan and Fayyad 2006).

At site 3, only a very small amount of dissolved Zn ($\sim$50 ppb) is measured at the peat surface. As for Cu, any Zn released by reductive dissolution of FMO at site 3 is likely to be removed quickly from the pore waters as it reacts with sulfides produced by sulfate reduction.

Major elements

Sodium is a conservative element and is therefore typically a good tracer for salinity. At sites 1, 2 and 3, Na increases with depth, especially near the surface (Fig. 1F). An increase in salinity is most likely due to evapotranspiration occurring at the surface and within the root zone. The Na profile at site 4 is quite distinct from those at the other sites, with nearly doubled Na levels between $\sim$5 cm and 20 cm depth. A large subsurface peak in salinity is unlikely to result from lateral advective flow of a saline water source, because it is not observed at the nearby sites. The most likely explanation for the spike in Na is enhanced evapotranspiration at this site relative to the others. Although site 4 is not more densely vegetated than the adjacent sites, the community structure of the vegetation is distinct from the others. In particular, this is the only site with duckweed (Table 1), suggesting that the duckweed (or perhaps some other vegetation unique to this site) enhances evapotranspiration near the surface.

The large subsurface peak in dissolved Na at site 4 is echoed by more muted increases in dissolved Ca, Mg and K, not observed at the other sites (Fig. 1C and D). This supports the idea that enhanced evapotranspiration occurs near the surface of this site relative to the other three. At all four sites, Ca and Mg increase with depth, typically at a greater rate than the increase with depth of dissolved Na. The region of rapidly increasing Ca and Mg roughly corresponds to the depths of decreasing pH. Speciation calculations suggest that the Ca and Mg profiles are controlled by carbonate mineral precipitation and dissolution. At sites 1, 2 and 4, calcite and aragonite are very close to saturation throughout the profiles (Fig. 13). Ordered dolomite is consistently supersaturated, but is unlikely to precipitate, due to slow kinetics. Disordered dolomite, and also magnesite ($MgCO_3$), are undersaturated at all four sites. At all sites, Ca and Mg are very well correlated ($R^2 \geq 0.90$), probably due to co-precipitation of

Table 3 Reaction stoichiometries and equilibrium constants used for thermodynamic calculations with the speciation software package JCHESS (van der Lee and de Windt 2000)

Reaction stoichiometry	Equilibrium constant
$Fe^{+3}_{(aq)} + HPO^{-2}_{4\,(aq)} + 2H_2O_{(l)} = FePO_4 \cdot 2H_2O_{(s)} + H^{+}_{(aq)}$ Strengite	log K = 11.3429
$5Ca^{+2}_{(aq)} + 3HPO^{-2}_{4\,(aq)} + H_2O_{(l)} = 4H^{+}_{(aq)} + Ca_5(PO_4)_3(OH)_{(s)}$ Hydroxylapatite	log K = 3.0746
$Ca^{+2}_{(aq)} + Mg^{+2}_{(aq)} + 2HCO^{-}_{3\,(aq)} = CaMg(CO_3)_{2(s)} + 2H^{+}_{(aq)}$ Ordered Dolomite	log K = −2.5135
$Ca^{+2}_{(aq)} + Mg^{+2}_{(aq)} + 2HCO^{-}_{3\,(aq)} = CaMg(CO_3)_{2(s)} + 2H^{+}_{(aq)}$ Disordered Dolomite	log K = −4.0579
$Mg^{+2}_{(aq)} + HCO^{-}_{3\,(aq)} = MgCO_{3(s)} + H^{+}_{(aq)}$ Magnesite	log K = −2.2936
$Ca^{+2}_{(aq)} + HCO^{-}_{3\,(aq)} = CaCO_{3(s)} + H^{+}_{(aq)}$ Aragonite	log K = −1.9931
$Ca^{+2}_{(aq)} + HCO^{-}_{3\,(aq)} = CaCO_{3(s)} + H^{+}_{(aq)}$ Calcite	log K = −1.8487
$Fe^{+2}_{(aq)} + HCO^{-}_{3\,(aq)} = FeCO_{3(s)} + H^{+}_{(aq)}$ Siderite	log K = 0.192
$Fe^{+2}_{(aq)} + HS^{-}_{(aq)} = FeS_{(s)} + H^{+}_{(aq)}$ Pyrrhotite	log K = 3.7193
$Fe^{+2}_{(aq)} + 0.25SO^{-2}_{4\,(aq)} + 1.75HS^{-}_{(aq)} + 0.25H^{+}_{(aq)} = FeS_{2(s)} + H_2O_{(l)}$ Pyrite	log K = 24.6534
$Mn^{+2}_{(aq)} + HCO^{-}_{3\,(aq)} = MnCO_{3(s)} + H^{+}_{(aq)}$ Rhodochrosite	log K = 0.1928

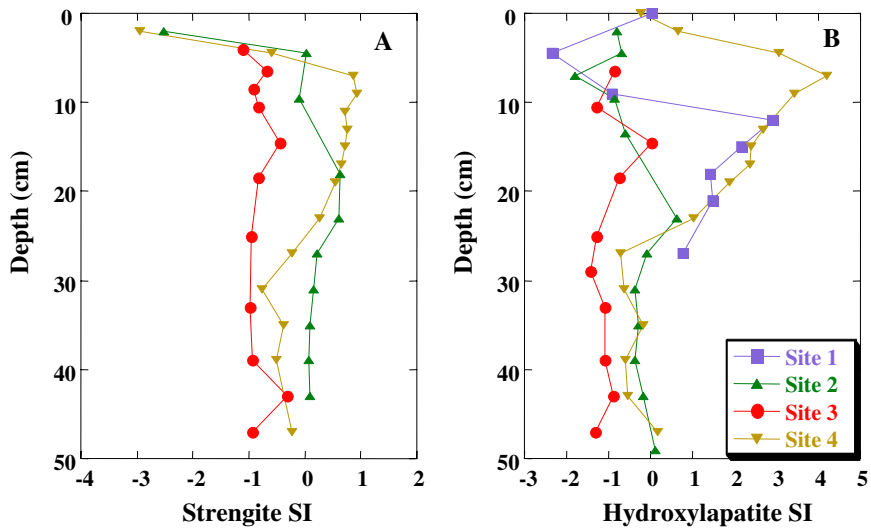

Fig. 12 Saturation indices as a function of depth at the four sites for (**A**) strengite ($FePO_4{\cdot}2H_2O$) and (**B**) hydroxylapatite ($Ca_5(PO_4)_3OH$) calculated using the speciation code JCHESS

both elements into dolomite, or more likely, in a solid solution of Mg with calcite or aragonite. Mg, and especially Ca, concentrations are lower at site 3 compared to the other sites. Although alkalinity levels are also lower at this site, dolomite, magnesite, calcite and aragonite are undersaturated at all depths.

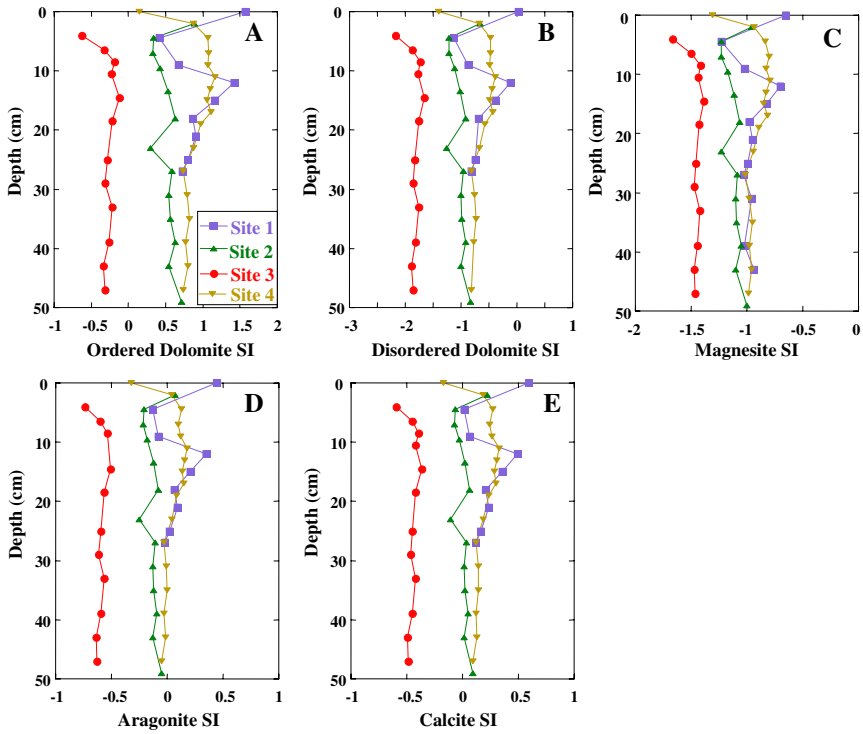

Fig. 13 Saturation indices as a function of depth at the four sites for (**A**) ordered dolomite ($CaMg(CO_3)_2$), (**B**) disordered dolomite ($CaMg(CO_3)_2$), (**C**) magnesite ($MgCO_3$), (**D**) aragonite ($CaCO_3$) and (**E**) calcite ($CaCO_3$) calculated using the speciation code JCHESS

In contrast to Na, Mg and Ca, dissolved K decreases with depth (Fig. 1E). K is produced by decaying organic matter, but may be taken up by macrophyte roots. In addition, K can be removed from the pore waters by sorption to clay minerals. The peak in dissolved K at ~8 cm depth at site 4 corresponds to the increase in dissolved Na and is likely due to a sharp change in salinity at this depth.

Solid phase metal distributions

Metal distributions inferred from operationally defined sequential extraction procedures must be regarded with some caution. Because these methods are operational in nature, it can be difficult to compare results from different extraction schemes (Quevauviller 1998; Filgueiras et al. 2002; Koretsky et al. 2006b). Furthermore, artifacts like redistribution of elements between phases can be introduced during soil or sediment preservation (Filgueiras et al. 2002). Extraction steps can remove more than just the target phase, or can incompletely dissolve target phases (Filgueiras et al. 2002). Nonetheless, useful information can often be gleaned from these procedures, particularly in comparisons of similar sites assessed using identical extraction procedures (Koretsky et al. 2006a, b; CM Koretsky et al. submitted).

Iron

Most of the solid phase iron is extracted with the reducible and oxidizable fractions (Fig. 2), consistent with primary association of solid phase iron with organic matter, iron oxides and iron sulfides. Much less iron is extracted with the exchangeable or carbonate phases. Siderite ($FeCO_3$) is significantly undersaturated at site 3 (Fig. 14A). At sites 2 and 4, and especially at site 1, siderite is much closer to saturation and may form a minor phase in the peat. Hjorth (2004) demonstrates that freeze-drying can mobilize Fe, probably present as poorly crystalline siderite, from the operationally-defined exchangeable/carbonate phase to the reducible fraction. This may explain why relatively little iron is extracted with the carbonates phase at sites 1, 2 and 4, in spite of the fact that siderite is close to saturation.

Reducible iron is generally presumed to be predominantly composed of iron oxides. However, previous studies have shown that freeze-drying can

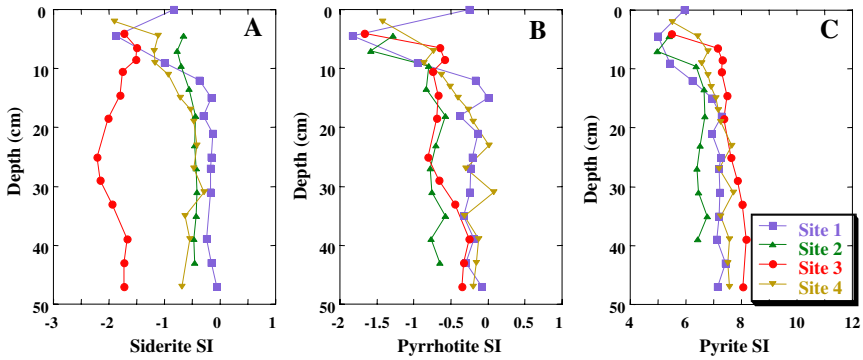

Fig. 14 Saturation indices as a function of depth at the four sites for (**A**) siderite ($FeCO_3$), (**B**) pyrrhotite (FeS) and (**C**) pyrite (FeS_2) calculated using the speciation code JCHESS

mobilize not only poorly crystalline siderite into this fraction, but can also lead to partial oxidation and release of iron sulfides in the reducible fraction (Rapin et al. 1986; Hjorth 2004). There is also some evidence that the reducible fraction may partially extract some organic-matter associated species as well (Filgueiras et al. 2002). However, the measured distribution of iron in the reducible phase at the four sites is entirely consistent with the redox stratification and organic matter degradation pathways inferred from the pore waters. That is, the extractions suggest labile Fe(III) oxide formation in the oxic zone, or possibly within oxic rhizospheres, and subsequent reductive dissolution of these solids via dissimilatory iron reduction, and perhaps also via abiotic chemical reduction, for example, coupled to sulfide oxidation. Thus, Fe extracted in the reducible fraction decreases with depth, especially at sites 1, 2 and 4, where Fe(III), and perhaps Mn(IV) reduction, are inferred to be more significant organic matter degradation pathways deeper in the sediments than at the mostly sulfidic site 3.

The largest pool of iron is extracted with the oxidizable fraction (Fig. 2). This iron is likely associated with a mixture of organic matter, iron monosulfides and iron disulfides (Koretsky et al. 2006a, b). Speciation calculations indicate that pyrrhotite (FeS) is undersaturated at all four sites in the upper 10 cm of the peat, but approaches saturation with increasing depth (Fig. 14B). However, it is much more likely that iron monosulfide phases including greigite, mackinawite or amorphous FeS (not included in the JCHESS thermodynamic database) will occur, rather than pyrrhotite, which is not often found in soil or sediments (Schoonen 2004). Pyrite (FeS_2) is significantly supersaturated at all depths, as has been reported for many other anoxic systems (Wersin et al. 1991; Schoonen 2004; Koretsky et al. 2006b; CM Koretsky et al. submitted).

In spite of the close proximity of the four sites, there are distinct differences in the oxidizable Fe distribution. At site 1, oxidizable Fe increases at the bottom of the core, presumably due to formation of iron sulfides only after labile iron oxide, which the reducible extraction suggests is elevated in the upper layers, is depleted. At site 3, where the pore water geochemistry is most compressed, with mostly sulfidic pore waters, the highest concentrations of oxdizable-Fe are found in the upper portion of the core. This is consistent with formation of Fe sulfides at much shallower depths at this site compared to the others. Site 4 is lacking some key depth data, but appears to be intermediate, with formation of iron sulfides at intermediate depths, again consistent with the intermediate redox stratification observed in the pore waters (i.e., less Fe(II) and Mn(II) than site 1, but more than site 3).

Manganese

Under oxic conditions, Mn forms Mn(IV) oxides, which can be important reservoirs for trace metals, especially Co, Zn and Cr (Davison 1993; Tonkin et al. 2004). Under suboxic conditions, Mn(IV) oxides reductively dissolve, releasing dissolved Mn(II). If this Mn does not diffuse into oxic zones near the surface or in the rhizosphere to be reoxidized, it is often removed from the pore waters into carbonate phases, including rhodochrosite (Davison 1993; LaForce et al. 2002). Under sulfidic conditions, at high degrees of pyritization, Mn can also be incorporated into sulfides (Morse and Luther 1999).

A lithophile element, Mn is not typically found in association with organic matter (Davison 1993). Some studies suggest that freeze-drying may mobilize Mn from the carbonate or exchangeable fractions into the reducible fraction (Rapin et al. 1986; Kersten and Forstner 1986), although other studies do not show this redistribution (Hjorth 2004). If such remobilization occurred in this study, it must have influenced only a small proportion of the carbonate and exchangeable Mn, as these are typically found in greater concentration than reducible Mn (Fig. 3).

The small proportion of Mn extracted in the oxidizable fraction does not vary substantially with depth or between sites (Fig. 3). This fraction of the Mn may be associated with sulfide minerals, or with the abundant organic matter in this peat. A larger quantity of Mn is extracted with the reducible fraction. The significant decrease in reducible-Mn with depth, especially between the upper 5 cm and the deeper peat, is consistent with reductive dissolution of Mn(IV) oxides. The remaining reducible-Mn may occur in microniches, such as oxic rhizospheres, or perhaps is contributed by partial redistribution of elements during freeze-drying or by non-target extraction of organic-matter associated Mn. The carbonate associated Mn is probably indicative of rhodochrosite formation, despite the fact that speciation calculations indicate undersaturation with respect to rhodochrosite at all four sites (Fig. 15). In a seasonal study of Mn in a palustrine emergent wetland, LaForce et al. (2002) used EXAFS to demonstrate the rhodochrosite was always the dominant Mn-bearing phase, although thermodynamic calculations did not always indicate saturation or supersaturation with respect to rhodochrosite. A surprisingly large proportion of the Mn is extracted with the exchangeable fraction, especially at site 4. Significant variability in the quantity of readily exchangeable Mn present at the four sites may be due to differences in macrophyte uptake of Mn. For example, *Scirpus littoralis* has been shown to efficiently translocate Mn from soils into roots, and to a lesser extent, shoots (Bhattacharya et al. 2006).

Barium

Barium, like Mn, is a lithophile element, and the distribution of Ba between the extracted phases is similar to that of Mn (Fig. 4). A relatively small

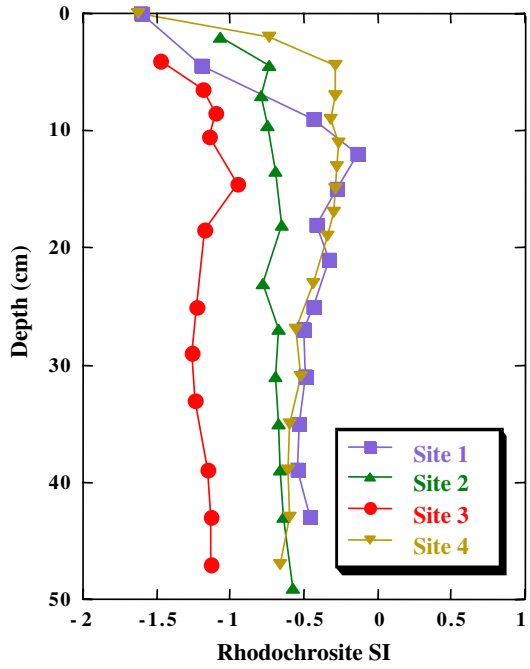

Fig. 15 Saturation indices as a function of depth at the four sites for rhodochrosite ($MnCO_3$) calculated using the speciation code JCHESS

quantity of Ba is present in the oxidizable fraction, and like Mn, it does not vary much with depth or site. This fraction of Ba tends to correlate well with oxidizable Zn (R^2 = 0.76, 0.56. 0.67 at sites 1, 2 and 3, respectively) and Cr (R^2 = 0.54 at site 4, 0.79 at site 1) and sometimes correlates well with Co (R^2 = 0.73 at site 1), Cu (R^2 = 0.78 at site 3) or Ni (R^2 = 0.72 at site 4). Like Cr and Mn, Ba does not typically form sulfide minerals, so oxidizable-Ba is presumably associated mostly with organic matter. Previous studies have shown that Ba preferentially sorbs to Mn oxides, rather than Fe oxides (e.g. Manceau et al. 2007). Thus, Ba extracted in the reducible phase is likely associated with Mn oxides. However, only at site 4 is there a strong correlation (R^2 = .90) between reducible-Ba and Zn. The smallest quantity of reducible-Ba is extracted at site 3, consistent with the differences in redox stratification at the four sites. A significant proportion of Ba is extracted in the carbonates phase. Like Mn, Ba can be found in carbonate minerals, such as witherite ($BaCO_3$) or in solid solutions with strontianite ($SrCO_3$) or aragonite (Deer et al. 1996). At sites 2, 3 and 4, carbonate extractable Ba correlates very well with carbonate

extractable Ni (R^2 = 0.74, 0.65 and 0.84, respectively) and Co (R^2 = 0.65, 0.81 and 0.59, respectively). However, a strong correlation between carbonate extractable Mn and Ba is again found only at site 4 (R^2 = 0.97). As for Mn, large concentrations of Ba are extracted in the exchangeable fraction, particularly at site 4, thus both elements are likely extracted from the same phase.

Nickel

Pyrite and other disulfides often contain large quantities of Ni (Morse and Luther 1999; Schoonen 2004). The bulk of the extracted nickel is associated with the oxidizable phase (Fig. 5). At sites 1 and 3, there are reasonably good correlations between oxidizable Ni and Zn (R^2 = 0.86, 0.79), Cu (R^2 = 0.83, 0.61) and, to a lesser extent, Cr (R^2 = 0.63, 0.59), suggesting that these elements are all found in association in the same phase. Oxidizable Ni does not correlate with oxidizable Fe at any of the sites, which could be explained by the presence of Fe in several sulfide phases, not all of which contain Ni. Alternatively, Ni might occur in a mixture of sulfide and organic phases. Cr, in particular, is rarely associated with sulfides (Morse and Luther 1999), and Cu is very often found in association with organic matter (Achterberg et al. 1997; Kadlec and Keoleian 1986), so the correlations with these elements suggest that at least some of the oxidizable Ni is associated with organic matter. The much smaller proportion of Ni extracted with the reducible fraction is most likely associated with Mn oxides and possibly with organic matter. There is a strong correlation between reducible Ni and Mn at sites 1, 2 and 3 (R^2 = 0.85, 0.89 and 0.79, respectively), although surprisingly good correlations are also found with reducible Fe at these sites (R^2 = 0.96, 0.87 and 0.69, respectively). Many previous studies have shown that Ni has a strong affinity for sorption on Mn oxides (Tessier et al. 1996; Green-Pedersen et al. 1997; Kay et al. 2001; Tonkin et al. 2004; Manceau et al. 2007). Larsen and Postma (1997) showed that pyrite oxidation in aquifer sediments released Ni, which subsequently sorbed to Mn oxides. Possibly the strong correlations of reducible Fe and Ni are indicative of Fe and Ni release from a partially oxidized sulfide phase. Significant differences in the vertical distribution of oxidizable-Ni at sites 1, 2 and 4 are consistent with more release of Ni from Mn oxides in the upper layers of site 3, which has less reducible Ni than site 1, to form Ni sulfides, resulting in slightly higher levels of oxidizable Ni in the shallow peat at site 3. The small proportion of Ni extracted with the carbonate phase may be sorbed on carbonates as Ni does not typically form a discrete carbonate phase. Ni has been shown to sorb to carbonates, although the affinity of Ni for sorption on carbonates is smaller than for many other substrates, including FMO, clays and organics (Green-Pedersen et al. 1997). Reasonably good correlations between carbonate extractable Ni and Ba (R^2 = 0.74, 0.65 and 0.84 at sites 2, 3, and 4, respectively), suggest that the Ni is associated with the same carbonate phase as Ba. Several wetland species, including *Lemna* (Zayed et al. 1998), *Typha* (Demirezen and Aksoy 2004) and *Scirpus* (Bhattacharya et al. 2006) have been shown to take up Ni from soils or pore waters to differing degrees, but the relatively small differences in Ni concentration and distribution at the four sites appear to be primarily controlled by differences in redox stratification.

Zinc

Zinc is a chalcophile element that forms distinct sulfide phases under anoxic conditions (Davison 1993; Morse and Luther 1999; Huerta-Diaz et al. 1993, 1998; Achterberg et al. 1997; Bostick et al. 2001). Some previous studies have suggested that freeze-drying or aeration of anoxic soils or sediments may mobilize Zn from sulfides into exchangeable, carbonate or reducible fractions (Rapin et al. 1986; Hjorth 2004; Kersten and Forstner 1986), although this is not always observed (Bordas and Bourg 1998). Most of the Zn in this study is extracted in the reducible or oxidizable phases, so a significant mobilization to the carbonate or exchangeable phases did not occur. However, oxidation of Zn-bearing sulfides during freeze-drying, with subsequent mobilization of Zn into the reducible fraction cannot be ruled out.

Oxidizable Zn typically correlates reasonably well with oxidizable Ba (R^2 = 0.73, 0.67 and 0.56 at sites 1, 3 and 4). At sites 2 and 4, there is also a good correlation with oxidizable Cr (R^2 = 0.82 and 0.80), which suggests that the oxidizable Zn is not primarily present in a sulfide phase. Zn can also be found in association with organic matter (Achterberg et al.

1997; El Bilali et al. 2002), which could explain the correlation with the oxidizable fractions of the lithophiles Ba and Cr. At site 1, the oxidizable portion of the Zn also correlates very well with oxidizable Ni (R^2 = 0.86) and Co (R^2 = .95), and reasonably well with Cu (R^2 = 0.68). At site 3, there is a stronger correlation with Cu (R^2 = 0.86) and less correlation with Ni (R^2 = 0.79), and a greater proportion of the Zn is extracted with the oxidizable phase, compared to sites 1 or 4. This is consistent with liberation of Zn from reductively dissolving FMO to form Zn sulfides with sulfide produced via sulfate reduction. A recent XAS study of Zn in a contaminated freshwater wetland demonstrated that Zn cycles seasonally between predominant association with FMO during dry, oxidizing conditions and association with sulfides and carbonates during flooded, anoxic conditions (Bostick et al. 2001). Peltier et al. (2003) also observed release of Zn from FMO during reductive dissolution into pore waters, followed by precipitation into sulfides. A similar cycle is suggested in this study by the larger proportion of oxidizable Zn at site 3, the site with the most compressed redox stratification, and by the decrease in reducible Zn observed with depth, particularly at sites 1 and 2 (Fig. 6). The small quantity of Zn in the carbonate phase correlates well with Cu and Co at site 1 (R^2 = 0.93, and 0.80), but not at the other sites. Differences in the total quantity of extracted Zn may reflect the different redox conditions at the four sites, as well as differential uptake of Zn by the heterogeneous vegetation. Many wetland macrophytes can translocate Zn from soils into roots and shoots, including *Phragmites* (Ye et al. 1998a; Peltier et al. 2003), *Scirpus* (Bhattacharya et al. 2006), and *Typha* (Ye et al. 1997, 1998b). FMO plaques formed in the rhizosphere have also been shown to sequester Zn (Zhang et al. 1998; Ye et al. 1998b; Hansel et al. 2001).

Lead

Under anoxic conditions Pb, which is a chalcophile element, forms distinct sulfide phases (Morse and Luther 1999; Huerta-Diaz et al. 1993, 1998), and also binds strongly to organic matter (Waaren and Haack 2001). Nearly all of the Pb in this study is extracted with the oxidizable fraction (Fig. 7). Although freeze-drying can shift Pb from the oxidizable fraction to the exchangeable, carbonate or reducible fractions (Hjorth 2004; Bordas and Bourg 1998), presumably due to oxidation of Pb-bearing sulfides, no such redistribution is observed here. Both the total quantity and the depth distribution of oxidizable Pb varies substantially between sites. Much more oxidizable Pb is extracted in the upper layers of site 3, the site with the most compressed pore water redox stratification. This is similar to observed variations in oxidizable-Fe and is consistent with precipitation of Pb sulfides in the near surface peat as sulfide is generated by microbial sulfate reduction. In contrast, and again similar to observations for oxidizable-Fe, most of the oxidizable Pb at site 1 is extracted from the deeper peat, again, consistent with the less compressed pore water redox stratification at this site and the greater inferred contribution of dissimilatory Fe(III) and Mn(IV) reduction to organic matter degradation in the near surface peat layers at this site compared to site 3. The elevated oxidizable Pb concentrations in the uppermost layers of site 1 are likely due to Pb association with organic matter deposited near the top of the peat profile (e.g. Fig. 11). At site 4, oxidizable Pb levels are elevated at shallower depths than at site 1, but deeper than at site 3, as for Fe, and again consistent with the intermediate pore water redox stratification at this site. Few correlations are found between Pb and other elements liberated in the oxidizable fraction at sites 1 and 4, suggesting that Pb forms a discrete sulfide phase or is found in a combination of sulfide and organic phases at these sites. Good correlations between oxidizable Pb and Zn (R^2 = 0.72) or Cu (R^2 = 0.85) at site 3 may indicate that these elements are associated with the same sulfide and/or organic phases. The very small fraction of extracted Pb associated with the carbonate phase varies little with depth or site. This Pb may be present as a discrete phase (i.e., cerrusite, $PbCO_3$), or more likely, exists in solid solution with or sorbed to aragonite or another carbonate phase. Differences in extracted Pb concentrations at the sites may also reflect differential uptake of Pb by macrophytes. Marsh vegetation including *Phragmites* (Ye et al. 1998b; Peltier et al. 2003), *Typha* (Ye et al. 1997, 1998a; Demirezen and Aksoy 2004), *Scirpus* (Bhattacharya et al. 2006) and *Lemna* (Zayed et al. 1998) have been demonstrated to translocate varying amounts of Pb from wetland soils into plant tissue.

Copper

Copper, like lead, is a chalcophile that forms discrete sulfide minerals (Balistrieri et al. 1992b; Achterberg et al. 1997; Morse and Luther 1999) or may associate with pyrite (Huerta-Diaz et al. 1993; Achterberg et al. 1997; Schoonen 2004) or FeS (Balistrieri et al. 1992b). Copper also has an affinity for organic matter, with which it forms very strong complexes (Kadlec and Keoleian 1986; Achterberg et al. 1997; El Bilali et al. 2002). Freeze-drying can oxidize Cu-bearing sulfides and mobilize Cu from the oxidizable fraction into the exchangeable or carbonate (Rapin et al. 1986) or reducible (Kersten and Forstner 1986; Hjorth 2004; Bordas and Bourg 1998) fractions. The majority of the copper in this study is found in association with the oxidizable fraction, so sulfide oxidation and subsequent mobilization of Cu into other fractions apparently does not affect the bulk of the extracted Cu (Fig. 8). The differences in oxidizable Cu depth distributions at sites 1, 3 and 4 are consistent with the redox stratification and depth distributions discussed for Pb and Fe. At site 3, with the most compressed pore water redox stratification, more oxidizable Cu is found in the upper layers of the peat, presumably due to formation of Cu-bearing sulfides. The correlation between oxidizable Cu and Pb at this site is very strong (R^2 = 0.85), as is the correlation with Zn (R^2 = 0.86), suggesting that these elements are found in the same phase. Oxidizable Cu correlates more strongly with Ni (R^2 = 0.83) at site 1, where most of the sulfide deposition is inferred to occur deeper than at site 3. The small quantity of reducible Cu is nearly invariant with site or depth and is quite close to detection limits. This reducible Cu may be the result of oxidation of a Cu-bearing sulfide during the freeze-drying process or extraction of non-target organic-associated Cu or it may indicate association of Cu with FMO. Previous studies have shown that Cu is sometimes found in association with FMO, typically forming ternary complexes with organic matter (Tessier et al. 1996; Achterberg et al. 1997). The distribution of Cu in the peat may also be influenced by macrophyte uptake. Previous studies have shown that *Phragmites* (Batty et al. 2000), *Lemna* (Zayed et al. 1998) and *Scirpus* (Bhattacharya et al. 2006) can translocate Pb from wetland soils.

Cobalt

Cobalt is a siderophile, frequently found in association with Fe. In anoxic soils or sediments, Co can form a discrete phase (CoS) or may be associated with disulfides including pyrite and marcasite (Huerta-Diaz et al. 1993, 1998; Morse and Luther 1999; Schoonen 2004). In oxic or suboxic soils or sediments, Co typically associates with oxides, including both Fe and Mn oxides (Balistrieri et al. 1992b; Davison 1993; Kay et al. 2001). In this study, Co occurs at low levels, near or below detection limits for all but the oxidizable fraction (Fig. 9). Differences in the depth distribution of oxidizable Co among the sites is consistent with that observed for other metals and suggests that Co sulfides precipitate at relatively shallow depths at site 3, deeper in the peat at site 1 and at intermediate depths at site 4. However, a good correlation between oxidizable Co and Cr at site 1 (R^2 = 0.86) and site 3 (R^2 = 0.83) does indicate that some of the Co may be associated with organics, as Cr is less likely to be found in a sulfide phase. A very small quantity of Co is found in the carbonate phase, which may indicate sorption on a more abundant carbonate phase or perhaps mobilization from the sulfides fraction during freeze-drying.

Chromium

Chromium, like Ba and Mn, is a lithophile element and is generally not associated with sulfides (Huerta-Diaz et al. 1998; Morse and Luther 1999). In anoxic soils or sediments, it is usually associated with organic matter (Otero and Macias 2003). Under suboxic or oxic conditions, Cr is typically sorbed to FMO (Balistrieri et al. 1992b; Davison 1993; Achterberg et al. 1997). Kersten and Forstner (1986) have shown that freeze-drying may mobilize Cr into the exchangeable fraction from either carbonate or reducible fractions. Such mobilization clearly did not occur in these samples, as Cr levels in both the exchangeable and carbonate fractions were consistently below detection limits (Fig. 10). Given the lack of affinity of Cr for sulfide minerals, it is somewhat surprising that oxidizable Cr correlates well with Zn (R^2 = 0.82 at site 1, 0.80 at site 4) and Co (R^2 = 0.86 at site 1, 0.83 at site 3) and that differences in the

depth distribution of oxidizable Cr at the sites are similar to those observed for Fe and the chalcophile elements Pb, Zn, and Cu. At site 1, there is a decrease in the reducible Cr concentration between the upper most samples and the deeper peat, as observed for reducible Mn. This may indicate release of Cr from a reductively dissolving Mn oxide phase, although a similar pattern is not observed at sites 2 and 4. Reducible Cr and Mn correlate well at sites 1 and 2 (R^2 = 0.81 and 0.80, respectively) suggesting that Cr is associated with a Mn oxide phase. Reducible Cr and Zn also show a weak correlation (R^2 = 0.51, 0.60 and 0.69). Like Cr, Zn is found in association with Mn oxides (e.g., Manceau et al. 2007).

Temporal comparisons

Pore water redox stratification was assessed in an earlier study (Koretsky et al. 2006a) as a function of season, at sites located quite to those chosen in this study. As noted in the field sites section, there are striking visual differences in the sites between the 2001–2002 study (Koretsky et al. 2006a) and this study. In 2006, the sites are drier with much denser and taller vegetation. Comparisons of the pore water data collected in this study during July 2006 with pore water data from June and September 2002 highlight some of the geochemical changes. pH, sulfate, ammonium and phosphate profiles are impacted very little by the apparent shifts in vegetation and hydrology. In contrast, at sites 1, 2 and 4, alkalinity, Fe(II), Fe(III) are considerably higher than in summer 2002 and dissolved sulfide concentrations are much lower. In contrast, alkalinity, Fe(II), Fe(III), and sulfide profiles at site 3 are very similar to those from summer 2002. This is consistent with denser vegetation leaking more oxygen into the subsurface, resulting in relatively more oxidized pore waters at sites 1, 2 and 4.

Koretsky et al. (2006a) used Tessier extractions on peat collected during March and June 2002 to examine the distribution of several metals among the carbonate, reducible and oxidizable phases. Total concentrations of Fe extracted in 2002 were somewhat lower than in this study, with maximum extractable Fe of $\sim$5 mg/g dry soil. The distribution of Fe among the phase and the depth distribution of extracted Fe was similar to that found in this study, with most of the Fe extracted in the oxidizable fraction and a lesser quantity in the reducible fraction. The distribution of Fe measured in June 2002 was most similar to the depth distribution of extracted Fe found in this study at site 3, consistent with the similarities in the pore water data. The quantity and depth distribution of Mn extracted in the reducible and oxidizable fractions in this study is also quite similar to that reported for peat collected in March 2002. However, much higher concentrations of carbonate extractable Mn, particularly in the uppermost peat (up to 600 μg/g dry soil) are reported by Koretsky et al. (2006a). These higher levels of carbonate-extractable Mn may reflect seasonal variability in Mn distributions, as discussed for an emergent palustrine wetland by LaForce et al. (2002).

The distribution of Zn among the operationally defined phases is similar in both studies. In the near surface peat, the total extractable Zn measured in June 2002 is comparable to levels measured in this study at sites 1 and 3. However, a much steeper decrease in both reducible and oxidizable Zn occurs with depth in the 2002 study, both during March and June. Similarly, there are comparable levels of Pb measured in the 2002 study, with the majority of the Pb associated with the oxidizable fraction, as in this study. However, the depth distribution of Pb in 2002 was again quite distinct from this study, with much more Pb near the top of the peat profile and a much more pronounced decrease with depth. There is also a large quantity of Pb extracted with the carbonate phase in the 2002 study relative to this study. Cu follows the same trend as Pb and Zn: overall concentrations and distribution among operationally-defined phases are similar to this study, but there is much more Cu extracted in the upper samples, and less in the deeper peat. All of these differences are consistent with the relatively more oxidized conditions in the shallow pore waters of three of the sites in 2006.

Both Co and Cr levels were considerably lower in the 2002 study (Koretsky et al. 2006a). For Co, <1 μg/g dry soil was reported, although the depth distributions and the proportion of Co associated with the various fractions are similar in both studies. For Cr, both studies suggest that the majority of the Cr is associated with the oxidizable fraction, but proportionally more reducible-associated Cr is found in the present study.

Conclusions

This study clearly demonstrates that both the pore waters and solid phase of minerotrophic fens are strongly redox stratified. Remarkable differences in redox stratification were observed at four adjacent sites with differing macrophyte species and densities. Specifically, the only site vegetated by the exotic invasive purple loosestrife had much more compressed redox stratification, with more reducing conditions in the pore waters and solid phase closer to the surface, compared to the adjacent three sites. Trace metal distributions at the four sites inferred from an operationally-defined sequential extraction method are consistent with pore water geochemistry. The more compressed redox stratification of pore waters at the loosestrife site was echoed in the increased levels of Fe, Pb, Cu, Ni, Zn, Co and Cr in the oxidizable fraction of the peat in the upper sediments at this site relative to metal concentrations and distributions at the adjacent sites. This study highlights the potential importance of small-scale variability in vegetation on peat biogeochemistry. Further study will be required to determine whether purple loosestrife or some other factor is responsible for the observed heterogeneity in the peat biogeochemistry. Comparisons with pore water and solid phase geochemistry measured at these same sites in 2002, when sites were wetter and had sparser vegetation, suggests that increased vegetation density generally leads to more oxidized conditions in both the pore waters and the solid phase, with significant remobilization of trace metals occurring in response to changes in redox. The comparison also highlights the potential importance of interannual variations in climate. The geochemistry of this minerotrophic fen varies tremendously both spatially and temporally. Such variations must be considered when limited, small-scale measurements of marsh biogeochemistry are extrapolated to different, and typically much larger, spatial and temporal scales.

Acknowledgments The authors gratefully acknowledge the support of the National Science Foundation CAREER program (NSF EAR 0348435). This grant allowed CMK to offer a summer wetlands field course, during which LB, AC, MH, TS, and MW completed much of the sampling and analytical work presented here. The authors also wish to thank Drs. Tsigabu Gebrehiwet and RV Krishnamurthy for providing the mannometric organic carbon measurements for site 3.

References

Achterberg EP, van den Berg CMG, Boussemart M, Davison W (1997) Speciation and cycling of trace metals in Esthwaite Water: a productive English lake with seasonal deep-water anoxia. Geochim Cosmochim Acta 61:5233–5253

Allen HE, Hall RH, Brisbin TD (1980) Metal speciation. Effects on aquatic toxicity. Environ Sci Technol 14:441–443

Arheimer B, Wittgren HB (2002) Modelling nitrogen removal in potential wetlands at the catchment scale. Ecol Eng 19:63–80

Balistrieri LS, Murray JW, Paul B (1992a) The cycling of iron and manganese in the water column of Lake Sammamish, Washington. Limnol Oceanogr 37:510–528

Balistrieri LS, Murray JW, Paul B (1992b) The biogeochemical cycling of trace metals in the water column of Lake Sammamish, Washington: response to seasonally anoxic conditions. Limnol Oceanogr 37:529–548

Batty LC, Baker AJM, Wheeler BD (2002) Aluminium and phosphate uptake in *Phragmites autralis*: the role of Fe, Mn and Al root plaques. Annal Bot 89:443–449

Batty LC, Baker AJM, Wheeler BD, Curtis CD (2000) The effect of pH and plaque on the uptake of Cu and Mn in *Phragmites australis* (Cav.) Trin Ex. Stuedel. Annal Bot 86:647–653

Berner RA (1980) Early diagenesis: a theoretical approach. Princeton University Press, Princeton, NJ

Bhattacharya T, Banerjee DK, Gopal B (2006) Heavy metal uptake by *Scirpus littoralis* schrad. from fly ash dosed and metal spiked soils. Environ Monit Assess 121:363–380

Blodau C, Mayer B, Peiffer S, Moore TR (2007) Support for an anaerobic sulfur cycle in two Canadian peatland soils. J Geophys Res Biogeosci 112:G02004

Bordas F, Bourg ACM (1998) A critical evaluation of sample pretreatment for storage contaminated sediments to be investigated for the potential mobility of their heavy metal load. Water Air Soil Pollut 103:137–149

Bostick BC, Hansel CM, Force MJL, Fendorf S (2001) Seasonal fluctuations in zinc speciation within a contaminated wetland. Environ Sci Technol 35:3823–3829

Boudreau BP (1999) Metals and models: diagenetic modelling in freshwater lacustrine sediments. J Paleolimnol 22:227–251

Brendel PJ, Luther GW (1995) Development of a gold amalgam voltammetric microelectrode for the determination of dissolved Fe, Mn, O_2, and S(-II) in porewaters of marine and freshwater sediments. Environ Sci Technol 29:751–761

Brix H, Sorrell BK, Lorenzen B (2001) Are *Phragmites*-dominated wetlands a net source or net sink of greenhouse gases? Aquat Bot 69:313–324

Buechler RJ (1996) The effects of the Kalamazoo Station No. 4 on the nearby Kleinstuck Nature Preserve, MS Thesis, Western Michigan University

Campbell PGC (1995) Interactions between trace metals and aquatic organisms: a critique of the free-ion activity model. In: Tessier A, Turner DR (eds) Metal speciation and bioavailability in aquatic systems. Wiley, New York

Choi JH, Park SS, Jaffe PR (2006) The effect of emergent macrophytes on the dynamics of sulfur species and trace metals in wetland sediments. Environ Pollut 140:286–293

Cooper DC, Picardal FF, Coby AJ (2006) Interactions between microbial iron reduction and metal geochemistry: effect of redox cycling on transition metal speciation in iron bearing sediments. Environ Sci Technol 40:1884–1891

Craft CB, Seneca ED, Broome SW (1991) Loss on ignition and Kjeldahl digestion for estimating organic carbon and total nitrogen in estuarine marsh soils: calibration with dry combustion. Estuaries 14(2):175–179

Crowder A (1991) Acidification, metals and macrophytes. Environ Pollut 71:171–203

Davison W (1993) Iron and manganese in lakes. Earth Sci Rev 34:119–163

Day JW, Ko JY, Rybczyk J, Sabins D, Bean R, Berthelot G, Brantley C, Cadoch L, Conner W, Day JN, Englande AJ, Feagley S, Hyfield E, Lane R, Lindsey J, Mistich J, Reyes E, Twilley R (2004) The use of wetlands in the Mississippi Delta for wastewater assimilation: a review. Ocean Coast Manag 47:671–691

Deer WA, Howie RA, Zussman J (1996) An introduction to the rock-forming minerals, 2nd edn. Prentice Hall

Deighton N, Goodman BA (1995) The speciation of metals in biological systems. In: Ure AM, Davidson CM (eds) Chemical speciation in the environment. Blackie Academic and Professional, New York

Demirezen D, Aksoy A (2004) Accumulation of heavy metals in *Typha angustifolia* (L.) and *Potamogeton pectinatus* (L.) living in Sultan Marsh (Kayseri, Turkey). Chemosphere 56:685–696

Dise N, Verry ES (2001) Suppression of peatland methane emission by cumulative sulfate deposition in simulated acid rain. Biogeochemistry 53:143–160

Doyle M, Otte ML (1997) Organism-induced accumulation of iron, zinc, and arsenic in wetland soils. Environ Pollut 96:1–11

Dzombak DA, Morel FMM (1990) Surface complexation modeling: hydrous ferric oxide. Wiley, New York

El Bilali L, Rasmussen PE, Hall GEM, Fortin D (2002) Role of sediment composition in trace metal distribution in lake sediments. Appl Geochem 17:1171–1181

Ellis CJ, Rochefort L (2006) Long-term sensitivity of a High Arctic wetland to Holocene climate change. J Ecol 94:441–454

Filgueiras AV, Lavilla I, Bendicho C (2002) Chemical sequential extraction for metal partitioning in environmental solid samples. J Environ Monit 4:823–857

Fredrickson JK, Zachara JM, Kukkadapu RK, Gorby YA, Smith SC, Brown CF (2001) Biotransformation of Ni-substituted hydrous ferric oxide by an Fe(III)-reducing bacterium. Environ Sci Technol 35:703–712

Froelich PN, Klinkhammer GP, Bender ML, Luedtke NA, Heath GR, Cullen D, Dauphin P, Hammond D, Hartman B, Maynard V (1979) Early oxidation of organic matter in pelagic sediments of the eastern equatorial Atlantic: suboxic diagenesis. Geochim Cosmochim Acta 43:1075–1090

Gambrell RP (1994) Trace and toxic metals in wetlands—a review. J Environ Qual 23:883–891

Gauci V, Fowler D, Chapman SJ, Dise NB (2004) Sulfate deposition and temperature controls on methane emission and sulfur forms in peat. Biogeochemistry 71:141–162

Green-Pedersen H, Jensen BT, Pind N (1997) Nickel adsorption on MnO_2, $Fe(OH)_3$, montmorillonite, humic acid and calcite: a comparative study. Environ Technol 18:807–815

Hamilton-Taylor J, Davison W (1995) Redox-driven cycling of trace elements in lakes. In: Lerman A, Imboden DM, Gat JR (eds) Physics and chemistry of lakes. Springer-Verlag

Hamilton-Taylor J, Smith EJ, Davison W, Zhang H (1999) A novel DGT-sediment trap device for the in situ measurement of element remobilization from settling particles in water columns and its application to trace metal release from Mn and Fe oxides. Limnol Oceanogr 44:1772–1780

Hansel CM, Fendorf S, Sutton S, Newville M (2001) Characterization of Fe plaque and associated metals on the roots of mine-waste impacted aquatic plants. Environ Sci Technol 35:3863–3868

Heiri O, Lotter AF, Lemcke G (2001) Loss on ignition as a method for estimating organic and carbonate content in sediments: reproducibility and comparability of results. J Paleolimnol 25:101–110

Hines ME, Evans S, Genthner BRS, Willis SG, Friedman S, Rooney-Varga JN, Devereux R (1999) Molecular phylogenetic and biogeochemical studies of sulfate-reducing bacteria in the rhizosphere of *Spartina alterniflora*. Appl Environ Microbiol 65:2209–2216

Hines ME, Knollmeyer SL, Tugel JB (1989) Sulfate reduction and other sedimentary biogeochemistry in a northern New England salt marsh. Limnol Oceanogr 34:578–590

Hogan DM, Jordan TE, Walbridge MR (2004) Phosphorus retention and soil organic carbon in restored and natural freshwater wetlands. Wetlands 24:573–585

Huerta-Diaz MA, Carignan R, Tessier A (1993) Measurement of trace metals associated with acid volatile sulfides and pyrite in organic freshwater sediments. Environ Sci Technol 27:2367–2372

Huerta-Diaz MA, Tessier A, Carignan R (1998) Geochemistry of trace metals associated with reduced sulfur in freshwater sediments. Appl Geochem 13:213–233

Hjorth T (2004) Effects of freeze-drying on partitioning patterns of major elements and trace metals in lake sediments. Anal Chim Acta 526:95–102

Jaynes ML, Carpenter SR (1986) Effects of vascular and nonvascular macrophytes on sediment redox and solute dynamics. Ecology 67:875–882

Jensen SI, Kuhl M, Glud RN, Jørgensen LB, Prieme A (2005) Oxygen microzones and radial oxygen loss from roots of *Zostera marina*. Mar Ecol Prog Ser 293:49–58

Johnston CA (1991) Sediment and nutrient retention by freshwater wetlands: effects on surface water quality. Crit Rev Env Control 21:491–565

Kadlec RH, Keoleian GA (1986) Metal ion exchange on peat. In: Fuchsman CH (ed) Peat and water. Elsevier

Kaldy JE, Eldridge PM, Cifuentes LA, Jones WB (2006) Utilization of DOC from seagrass rhizomes by sediment bacteria: ^{13}C-tracer experiments and modeling. Mar Ecol Prog Ser 317:41–55

Kay JT, Conklin MH, Fuller CC, O'Day PA (2001) Processes of nickel and cobalt uptake by a manganese oxide forming sediment in Pinal Creek, Globe Mining District, Arizona. Environ Sci Technol 35:4719–4725

Keller JK, Bridgham SD (2007) Pathways of anaerobic carbon cycling across an ombrotrophic-minerotrophic peatland gradient. Limnol Oceanogr 52(1):96–107

Keller BEM, Lajtha K, Cristofor S (1998) Trace metal concentration in the sediments and plants of the Danube Delta, Romania. Wetlands 18:42–50

Kerner M, Wallmann K (1992) Remobilization events involving Cd and Zn from intertidal flat sediments in the Elbe Estuary during the tidal cycle. Estuar Coast Shelf Sci 35:371–393

Kersten M, Forstner U (1986) Chemical fractionation of heavy metals in anoxic estuarine and coastal sediments. Water Sci Technol 18:121–130

Koretsky CM, Cappellen P, DiChristina TJ, Kostka JE, Lowe KL, Moore CM, Roychoudhury AN, Viollier E (2005) Salt marsh pore water geochemistry does not correlate with microbial community structure. Estuar Coast Shelf Sci 62:233–251

Koretsky CM, Haas JR, Ndenga NT, Miller D (2006a) Seasonal variations in vertical redox stratification and potential influence on trace metal speciation in minerotrophic peat sediments. Water Air Soil Pollut 173:373–403

Koretsky CM, Haas JR, Miller D, Ndenga NNT (2006b) Seasonal variations in pore water and sediment geochemistry of littoral lake sediments (Asylum Lake, MI, USA). Geochem Trans 7:11

Koretsky CM, Moore CM, Lowe KL, Meile C, DiChristina T, Cappellen P (2003) Seasonal oscillation of microbial iron and sulfate reduction in saltmarsh sediments (Sapelo Island, GA, USA). Biogeochemistry 64:179–203

Krishnamurthy RV, Syrup K, Long A (1999) Is selective preservation of nitrogeneous organic matter reflected in the $\delta^{13}C$ signal of lacustrine sediments? Chem Geol 158:165–172

LaForce MJ, Hansel CM, Fendorf S (2002) Seasonal transformations of manganese in a palustrine emergent wetland. Soil Sci Soc Am J 66:1377–1389

Larsen F, Postma D (1997) Nickel mobilization in a groundwater well field: release by pyrite oxidation and desorption from manganese oxides. Environ Sci Technol 31:2589–2595

Leermakers M, Gao Y, Gabelle C, Lojen S, Ouddane B, Wartel M, Baeyens W (2005) Determination of high resolution pore water profiles of trace metals in sediments of the Rupel River (Belgium) using DET (diffusive equilibrium in thin films) and DGT (diffusive gradients in thin film) techniques. Water Air Soil Pollut 166:265–286

Lovley DR, Phillips EJP (1986) Availability of ferric iron for microbial reduction in bottom sediments of the freshwater tidal Potomac River. Appl Environ Microbiol 52:751–757

Lowe KL, DiChristina TJ, Roychoudhury AN, Cappellen P (2000) Microbiological and geochemical characterization of microbial Fe(III) reduction in salt marsh sediments. Geomicrobiol J 17:1–16

Manceau A, Lanson M, Geoffroy N (2007) Natural speciation of Ni, Zn, Ba, and As in ferromanganese coatings on quartz using X-ray fluorescence, absorption and diffraction. Geochim Cosmochim Acta 71:95–128

Mendelssohn IA, Postek MT (1982) Elemental analysis of deposits on the roots of *Spartina alterniflora* Loisel. Am J Bot 69(6):904–912

Mitsch WJ, Gosselink JG (2000) Wetlands, 3rd edn. Wiley, New York

Mkandawire M, Taubert B, Dudel EG (2004) Capacity of *Lemna gibba* L. (duckweed) for uranium and arsenic phytoremediation in mine tailing waters. Int J Phytoremediation 6:347–362

Morse JW, Arakaki T (1993) Adsorption and coprecipitation of divalent metals with mackinawite (FeS). Geochim Cosmochim Acta 57:3635–3640

Morse JW, Luther GW (1999) Chemical influences on trace metal–sulfide interactions in anoxic sediments. Geochim Cosmochim Acta 63:3373–3378

Mungasavalli DP, Viraraghaven T (2006) Constructed wetlands for stormwater management: a review. Fresenius Environ Bull 15:1363–1372

Myers CR, Nealson KH (1988) Bacterial manganese reduction and growth with manganese oxide as sole terminal electron acceptor. Science 240:1319–1321

Norton SA (1987) The stratigraphic record of atmospheric loading of metals at the ombrotropic Big Heath Bog, Mt. Desert Island, Maine, USA. In: Hutchinson TC, Meerma KM (eds) Effects of atmospheric pollutants on forests, wetlands and agricultural ecosystems, NATO ASI Series, Vol G26, Springer-Verlag

Oporto C, Arce O, Broeck EVD, van der Bruggen B, Vandecasteele C (2006) Experimental study and modelling of Cr(VI) removal from wastewater using *Lemna minor*. Water Res 40:1458–1464

Otero XL, Macias F (2003) Spatial variation in pyritization of trace metals in salt-marsh soils. Biogeochemistry 62:59–86

Pedersen O, Borum J, Duarte CM, Fortes MD (1998) Oxygen dynamics in the rhizosphere of *Cymodocea rotundata*. Mar Ecol Prog Ser 169:283–288

Peltier EF, Webb SM, Gaillard JF (2003) Zinc and lead sequestration in an impacted wetland system. Adv Environ Res 8:103–112

Perkins SM, Filipelli GM, Slouch CJ (2000) Airborne trace metal contamination of wetland sediments at Indiana Dunes National Lakeshore. Water Air Soil Pollut 122:231–260

Quevauviller P (1998) Operationally defined extraction procedures for soil and sediment analysis. I. Standardization. Trends Anal Chem 17:289–298

Rapin F, Tessier A, Campbell PGC, Carignan R (1986) Potential artifacts in the determination of metal partitioning in sediments by a sequential extraction procedure. Environ Sci Technol 20:836–840

Rausch N, Ukonmaanaho L, Nieminen TM, Krachler M, Shotyk W (2005) Porewater evidence of metal (Cu, Ni, Co, Zn, Cd) mobilization in an acidic, ombrotrophic bog impacted by a smelter, Harjavalta, Finland and comparison with reference sites. Environ Sci Technol 39:8207–8213

Rickard D, Schoonen MAA, Luther GW (1995) Chemistry of iron sulfides in sedimentary environments. In: Geochemical transformations of sedimentary sulfur. American Chemical Society

Roden EE, Wetzel RG (1996) Organic carbon oxidation and suppression of methane production by microbial Fe(III) oxide reduction in vegetated and unvegetated freshwater wetland sediments. Limnol Oceanogr 41:1733–1748

Roden EE, Wetzel RG (2002) Kinetics of microbial Fe(III) oxide reduction in freshwater wetland sediments. Limnol Oceanogr 47:198–211

dos Santos Afonso M, Stumm W (1992) Reductive dissolution of iron(III) (hydr)oxides by hydrogen sulfide. Langmuir 8:1671–1675

Schoonen MAA (2004) Mechanisms of sedimentary pyrite formation. In: Amend JP, Edwards KJ, Lyons TW (eds) Sulfur biogeochemistry—past and present, vol. 379. Geological Society of America

Shindell DT, Walter BP, Faluvegi G (2004) Impacts of climate change on methane emissions from wetlands. Geophys Res Lett 31:L21202

Shotyk W (1988) Review of the inorganic geochemistry of peats and peatland waters. Earth Sci Rev 25:95–176

Shotyk W (1996) Natural and anthropogenic enrichments of As, Cu, Pb, Sb, and Zn in ombrotropic versus minerotrophic peat bog profiles, Jura Mountains, Switzerland. Water Air Soil Pollut 90:375–405

Shotyk W, Norton SA, Farmer JG (1997) Summary of the workshop on peat bog archives of atmospheric metal deposition. Water Air Soil Pollut 100:213–219

Smemo KA, Yavitt JB (2006) A multi-year perspective on methane cycling in a shallow peat fen in central New York state, USA. Wetlands 26:20–29

Sunda W, Guillard RRL (1976) The relationship between cupric ion activity and the toxicity of copper to phytoplankton. J Mar Res 34:511–529

Sweidan KA, Fayyad MK (2006) The use of duckweed for removal of heavy metals and organic compounds from wastewaters in As-samra. Fresenius Environ Bull 15:354–359

Tarnocai C (2006) The effect of climate change on carbon in Canadian peatlands. Glob Planet Change 53:222–232

Tessier A, Campbell PGC, Bisson M (1979) Sequential extraction procedure for the speciation of particulate trace metals. Anal Chem 51:844–851

Tessier A, Campbell PGC, Bisson M (1982) Particulate trace metal speciation in stream sediments and relationships with grain size: implications for geochemical exploration. J Geochem Explor 16:77–104

Tessier A, Fortin D, Belzile N, DeVitre RR, Leppard GG (1996) Metal sorption to diagenetic iron and manganese oxyhydroxides and associated organic matter: narrowing the gap between field and laboratory measurements. Geochim Cosmochim Acta 60:387–404

Tonkin JW, Balistrieri LS, Murray JW (2004) Modeling sorption of divalent metal cations on hydrous manganese oxide using the diffuse double layer model. Appl Geochem 19:29–53

Trettin CC, Laiho R, Minkkinen K, Laine J (2006) Influence of climate change factors on carbon dynamics in northern forested peatlands. Can J Soil Sci 86:269–280

Urban NR, Eisenreich SJ, Grigal DF (1989) Sulfur cycling in a forested *Sphagnum* bog in northern Minnesota. Biogeochemistry 7:81–109

Van Cappellen P, Wang Y (1996) Cycling of iron and manganese in surface sediments: a general theory for the coupled transport and reaction of carbon, oxygen, nitrogen, sulfur, iron and manganese. Am J Sci 296:197–243

van der Lee J, De Windt L (2000) CHESS tutorial and cookbook. User's guide Nr. LHM/RD/99/05 Fontainebleau. CIG-Ecole des Mines de Paris, France

Verhoeven JTA, Arheimer B, Yin C, Hefting MM (2006) Regional and global concerns over wetlands and water quality. Trends Ecol Evol 121:96–103

Warren LA, Haack EA (2001) Biogeochemical controls on metal behaviour in freshwater environments. Earth Sci Rev 54:261–320

Watson A, Nedwell DB (1998) Methane production and emission from peat: the influence of anions (sulphate, nitrate) from acid rain. Atmosph Env 32:3239–3245

Weis JS, Weis P (2004) Metal uptake, transport and release by wetland plants: implications for phytoremediation and restoration. Environ Int 30:685–700

Wersin P, Höhener P, Giovanoli R, Stumm W (1991) Early diagenetic influences on iron transformations in a freshwater lake sediment. Chem Geol 90:233–252

Wieder RK, Lang GE (1988) Cycling of inorganic and organic sulfur in peat from Big Run Bog, West Virginia. Biogeochemistry 5:221–242

Wieder RK, Yavitt JB, Lang GE (1990) Methane production and sulfate reduction in two Appalachian peatlands. Biogeochemistry 10:81–104

Wundeground (2007) http://www.wunderground.com/history/airport/KAZO/2006/7/15/MonthlyHistory.html, site visited May 2007

Yao W, Millero FJ (1996) Oxidation of hydrogen sulfide by hydrous Fe(III) oxides in seawater. Mar Chem 52:1–16

Ye ZH, Baker AJM, Wong MH, Willis AJ (1997) Zinc, lead and cadmium tolerance, uptake and accumulation by *Typha latifolia*. New Phytol 136:469–480

Ye Z, Baker AJM, Wong MH, Willis AJ (1998a) Zinc, lead and cadmium accumulation and tolerance in *Typha latifolia* as affected by iron plaque on the root surface. Aquat Bot 61:55–67

Ye ZH, Wong MH, Baker AJM, Willis AJ (1998b) Comparison of biomass and metal uptake between two populations of *Phragmites australis* grown in flooded and dry conditions. Annal Bot 82:83–87

Zachara JM, Fredrickson JK, Smith SC, Gassman PL (2001) Solubilization of Fe(III)oxide-bound trace metals by a dissimilatory Fe(III) reducing bacterium. Geochim Cosmochim Acta 65:75–93

Zayed A, Gowthaman S, Terry N (1998) Phytoaccumulation of trace elements by wetland plants: I. Duckweed. J Environ Qual 27:715–721

Zhang X, Zhang F, Mao D (1998) Effect of iron plaque outside roots on nutrient uptake by rice (*Oryza sativa* L.). Zinc uptake by Fe-deficient rice. Plant Soil 202:33–39